Department of Mathematics and Statistics

Theoretical Study of Calorimetric Measurements in Quantum Integrated Circuits

Brecht Donvil

Doctoral dissertation, to be presented for public examination with the permission of the Faculty of Science of the University of Helsinki in Auditorium PIII, Porthania, City Centre Campus, on the 1st of October, 2020 at 12 o'clock.

University of Helsinki
Finland

Supervisors

Paolo Muratore-Ginanneschi, University of Helsinki, Finland
Jukka Pekola, Aalto University, Finland

Pre-examiners

Wojciech De Roeck, KU Leuven, Belgium
Michele Campisi, University of Florence, Italy

Opponent

Joachim Ankerhold, Ulm University, Germany

Custos

Antti Kupiainen, University of Helsinki, Finland

Contact information

Department of Mathematics and Statistics
P.O. Box 68 (Pietari Kalmin katu 5)
FI-00014 University of Helsinki
Finland

ISBN 978-951-51-6572-5 (paperback)
ISBN 978-951-51-6573-2 (PDF)
Helsinki 2020
Unigrafia

Abstract

Recent developments in experimental methods allow for the study of thermodynamic properties of quantum systems. In quantum integrated circuits, quantum systems are elements in an electric circuit that can straightforwardly be coupled to other elements. This manipulability allows one to construct quantum heat engines, Maxwell demons etc. Quantum integrated circuits also are one of the main potential settings to realise a working quantum computer. Calorimetric measurements in integrated circuits serve as a promising technique to probe thermodynamic laws of the quantum regime and to study the inner workings of quantum devices.

Due to this experimental accessibility, the theoretical study of open quantum systems in the context of quantum integrated circuits is highly relevant. Open quantum systems are typically small systems, e.g. qubits or oscillators, in contact with one or more reservoirs. The research on which this thesis is based can roughly be divided into two parts.

The first part is concerned with the thermodynamics of a driven qubit in contact with a thermal bath. This system is the archetype of a quantum out-of-equilibrium system. In one case the qubit is strongly driven by a semiclassical driving field. Building on earlier works, the thermodynamic relations of the system are found by proving the equivalence with an easier to study qubit-oscillator system. In the other, case the qubit is driven by being in contact with two baths with a temperature gradient. The full generating function is derived in a proper approximative scheme and a fluctuation-dissipation relation is found.

The second part focusses on a specific experimental scheme to perform calorimetric measurements. The scheme relies on coupling a quantum system to a finite reservoir and performing fast temperature measurements on the reservoir. Doing so allows one to infer energy changes in the reservoir and therefore to obtain the heat exchanged with the system. The dynamics of this system are modelled for weak system-reservoir coupling and concrete experimental predictions are made. In new work, the dynamics for a toy model of a system interacting with a finite reservoir are derived from first principles for a specific model. The first principle derivation matches with the earlier modelled dynamics in the weak coupling and allows to consider strong system-reservoir coupling as well.

Acknowledgements

I would like to start by thanking my advisors: Paolo for supporting me over the past five years. For our many animated discussions and your seemingly endless patience with my questions. For showing me your vision on doing scientific research and physics in general. I have learned a great deal from you over the past five years. I owe you much gratitude and am thankful to have been able to work with you.

Jukka, thank you for letting me be part of your research and your group. I greatly enjoyed visiting you in Micronova every week. As a theorist, it was very enlightening to regularly come in contact with experiments and it made me grow as a researcher. Thank you for all your support and advice.

I thank my pre-examiners Wojciech De Roeck and Michele Campisi for carefully reading my thesis and giving their insightful comments and Joachim Ankerhold for kindly agreeing to be my opponent.

Antti, it was a pleasure to be part of your research group. Thank you for creating an environment where I was able to freely explore my research interests. Kay, you were a great support for me during my first years in Helsinki. You gave many useful pieces of advice in my first steps to becoming a researcher and helped me settle in at the department. Dima, I thank you for the many useful discussions we had. Your combined knowledge of theory and experiments was very helpful. The times we worked together were always very instructive. Bayan, thank you for being so kind and cheerful. Thank you for all your advice and help. Christian, perhaps I owe you the biggest thanks. Without you I would have never come to Helsinki and started this adventure. Christian and Wojciech, thank you for making me always feel welcome in Leuven.

I would like to thank all of my collaborators: Erik and Kirone; Lara, Tomaž and Toni.

Many thanks to the whole mathematical physics group at the university of Helsinki. Thank you to all the members of the PICO group at Aalto university

for making me feel part of your group. Visiting you always brightened up my week.

I want to thank all the friends I made in Helsinki. Francesca, Laura and Tatiana I want to thank you for teaching me the proper time to salt boiling water. Tatiana, I had a blast living with you, organising parties, inventing Belgian-Italian fusion cuisine that the world was not quite ready for and so much more. Thank you for always being there for me. Francesca, thank you for all the great times we had together in Helsinki, it was a pleasure serving under you in the OC. Nasibeh, you were a great friend from the moment I met you. Thank you for being there in difficult and in fun times. I hope I was as big of a support for you as you were for me. Many thanks to Joona for showing me the Finnish way of life and to Antti for teaching me the way of the beach. To Miriam who was one of the first persons I met in Helsinki, who helped me find my way in Helsinki, and has been a friend ever since. To Todd, for brightening up our Finnish classes. To Kalle, for sharing your passion of classical statistical mechanics and for teaching me the importance of the deadlift. To Petri, for teaching me Kumpula's history and to Rui, for teaching me the Bohmian way. Thank you Anna for being my unlicensed lawyer, a great office mate, and an even better friend.

Thank you, Marie doing the final proofread of my thesis and giving many helpful comments and interesting opinions.

I want to thank my friends in Belgium for making me feel like I never really left home.

Finally, I thank my family for their many visits, uncountable skype calls and unlimited support. The help you have given me over the past years is invaluable.

Helsinki, October 2020
Brecht Donvil

I think there are people that help you become the person that you end up being, and you can be grateful for them, even if they were never meant to be in your life forever.

-Diane Nguyen

List of Articles

I. Donvil B. Thermodynamics of a periodically driven qubit, Journal of Statistical Mechanics: Theory and Experiment, (2018) 043104

II. Donvil B., Muratore-Ginanneschi P., Pekola J. P. and Schwieger K. Model for calorimetric measurements in an open quantum system, Physical Review A 97, 052107 (2018)

III. Donvil B., Muratore-Ginanneschi P., Pekola J. P. Hybrid master equation for calorimetric measurements, Physical Review A 99, 052107 (2019)

IV. Aurell E., Donvil B. and Kirone M. Large Deviations and Fluctuation Theorem for the Quantum Heat Current, Physical Review E 101, 052116 (2020)

During his dissertation the author also contributed to the article [1], excluded from his thesis.

Author's Contribution

II. The author made fundamental contributions to all parts of the manuscript.

III. The author made fundamental contributions to all parts of the manuscript.

IV. The author made fundamental contributions to all parts of the manuscript.

Contents

Chapter 1

Introduction

The development of solid state quantum bits [2, 3], qubits, based on combining superconducting elements and the Josephson effect has led to a whole range of new experiments. These qubits, unlike microscopic qubits such as spins and atoms, are the result of the collective behaviour of many particles [4]. They are more easily manipulated and coupled to other systems than their microscopic counterparts. Due to these properties, superconducting qubits are one of the main candidates as building blocks for quantum computers. They were indeed used in the first experiment claiming to have achieved quantum supremacy [5]. The processor used in [5], named Sycamore, consists of 54 transmon qubits [6]. It outperformed a classical supercomputer in sampling outputs of pseudo-random quantum circuits. A task that took Sycamore 200 seconds to perform would take a classical supercomputer an estimated 10000 years.

In the development of genuine quantum devices one inevitably runs into the effects of their environment and, more specifically, heat exchange with it. For some applications, such as quantum computing, one aims to reduce effects of the environment as much as possible as it destroys coherences. In other cases one hopes to use heat to perform useful operations. Examples are heat engines [7, 8], where one aims to use heat current to perform useful work or Maxwell demons, where one transforms thermal fluctuations into work [9]. Alternatively, one can study the heat exchange between a device and its environment to probe the inner workings of the device and the foundations of quantum mechanics itself [10].

The research reported in Articles I-IV, which form the basis of this dissertation, is largely concerned with the latter. More concretely, Articles I-IV are dedicated to heat currents and calorimetric measurements in quantum integrated circuits, although the applicability of the results is not necessarily limited to this

context. Let us discuss the contents of the articles in more detail.

Articles I and IV focus on the heat current flowing between a qubit and its environment. In Article I the qubit is subject to strong driving in addition to being weakly coupled to a thermal environment. Based on earlier results for a non-interacting driven qubit [11, 12, 13, 14], an equivalence is developed between the dynamics of the strongly driven qubit and those of a qubit-oscillator system interacting with the thermal environment. Using this equivalence, the thermodynamic relations of the driven qubit are easily obtained from the qubit-oscillator system. Article IV concerns the generating function of the heat flowing through a qubit strongly coupled to multiple thermal environments. Under the so-called Non-Interacting Blip Approximation (NIBA) [15], an explicit expression for the generating function is found, recovering earlier results obtained using the polaron transform [16, 17].

Articles II & III are motivated by the setup proposed in [18] to perform calorimetric measurements of work in quantum integrated circuits. The setup consists of a superconducting qubit and a resistor which acts as a finite reservoir, a calorimeter. By accurately measuring the temperature of the resistor [19, 20, 21], one can probe the dynamics of the qubit. Articles II & III build upon an earlier work [22], which models the setup [18], to numerically and analytically study the behaviour of the resistor temperature. Additionally, we present new results in this dissertation: a first principle derivation for the joint dynamics of a system state and reservoir energy for a fermion interacting with a fermion bath. This derivation passes through the exact fermion-fermion dynamics and allows us to go beyond weak coupling.

This dissertation is structured as follows. Chapter 2 provides a short introduction to the dynamics of open quantum systems. For weakly coupled systems we present the Lindblad equation and related jumps equations. Also methods for strongly coupled system are discussed, including the results of Article IV. In Chapter 3 we introduce Floquet theory for driven quantum systems, which was used in Articles I & II. Additionally, the results of Article I are presented. Calorimetric measurements in integrated circuits are the subject of Chapter 4. The results of Articles II & III are discussed. Chapter 5 introduces multiscale perturbation theory, a method to solve partial differential equations. This technique was used extensively in Articles II & III . The use of multiscale perturbation over ordinary perturbation theory is shown with a motivating example. The results obtained by using multiscale perturbation from Articles II & III are discussed. In Chapter 6 we present a new derivation of a system-reservoir energy

hybrid master equation. We study a fermion interacting with a fermion bath. The fermion-fermion bath model is Gaussian, and as such, the dynamics can be integrated exactly. We study two limits for which we obtain an explicit hybrid master equation. Assuming weak system-reservoir coupling we obtain a master equation similar to the one studied in Article III. In the zero temperature limit we find a master equation valid at arbitrary coupling.

Chapter 2

Open Quantum Systems

The dynamics of a quantum system with Hamiltonian H are described by the Schrödinger equation. Let $\psi(t)$ be the wave function of the system at time t, $\psi(t)$ satisfies the differential equation

$$\frac{d}{dt}\psi(t) = -\frac{i}{\hbar}H\psi(t). \tag{2.1}$$

Equivalently, the density operator $\rho(t)$ of the system satisfies the Liouville-von Neumann equation

$$\frac{d}{dt}\rho(t) = -\frac{i}{\hbar}[H, \rho(t)]. \tag{2.2}$$

Imagine now that we are not interested in the whole system, but only in a component S. To calculate expectation values of operators acting on S, we do not need access to the whole state of the system. Instead, it is enough to only know the information related to S stored in the density matrix of the total system. For this purpose, let us define the reduced density operator $\rho_S(t)$ of the interesting component by taking the partial trace tr_R of $\rho(t)$ over the degrees of freedom of rest of the system

$$\rho_S(t) = \mathrm{tr}_R(\rho(t)). \tag{2.3}$$

Having access to the reduced density matrix allows us to calculate the expectation value of an operator A acting on the Hilbert space of S, as

$$\mathrm{tr}(A\,\rho(t)) = \mathrm{tr}_S(A\,\rho_S(t)), \tag{2.4}$$

where tr_S is the trace over the subsystem S.

By taking the partial trace on both sides of equation (2.2), we find that $\rho_S(t)$ satisfies the equation

$$\frac{d}{dt}\rho_S(t) = -\frac{i}{\hbar}\,\mathrm{tr}_R([H, \rho(t)]). \tag{2.5}$$

Since we only need the reduced density matrix, it would be convenient to have a closed equation for the dynamics of $\rho_S(t)$, instead of always having to pass through the state of the complete system $\rho(t)$. Concretely, we would like to have a linear operator $\mathcal{L}_t$, such that

$$\frac{d}{dt}\rho_S(t) = \mathcal{L}_t(\rho_S(t)). \tag{2.6}$$

Depending on the specific system, finding $\mathcal{L}_t$ is a non-trivial matter.

A major result obtained by Gorini, Kossakowski and Sudarshan [23] and Lindblad [24] (GKLS) determines the structure of $\mathcal{L}$, see also for example [25, 26]. In short, they derived the most general form of a Markovian evolution preserving the trace and completely positive for any initial condition. We recall that a map E is a completely positive map iff [27]

- $E(A)$ is positive for positive operators A
- For any finite extension of the Hilbert space on which A acts and $\mathbb{I}$ the identity operator on that extension, $(E \otimes \mathbb{I})(B)$ is positive for positive B acting on the extended space.

Under these conditions the generator $\mathcal{L}_t$ has the form

$$\mathcal{L}_t(\rho) = -i[H(t), \rho] + \sum_k \gamma_k(t)(V_k(t)\rho V_k^\dagger(t) - \frac{1}{2}\{V_k^\dagger(t)V_k(t), \rho\}), \tag{2.7}$$

where $H(t)$ is a Hermitian operator, $V_k(t)$ an operator and $\gamma_k(t) \geq 0$ for all k and t.

Although the result by GKLS determines the structure of $\mathcal{L}$, finding the operators H, V and the rates γ in practice is not straightforward. The so-called weak coupling limit [28, 29, 30], based on the Van Hove scaling limit [31], provides a well-defined rigorous limit in which the form (2.7) can be derived from an underlying microscopic model. The physical assumptions are that the system of interest is only weakly coupled to the environment and that the environment is much larger than the system. As a result of the weak coupling derivation, one finds that the generator of the unitary evolution in (2.7) $H(t)$ is the isolated

system Hamiltonian plus the so called Lamb Shift. The Lindblad operators $V_k(t)$ are eigenoperators of the system Hamiltonian and as such induce transitions between energy levels of the system.

We will not discuss the weak-coupling derivation here. In the next section we examine a quantum jump process induced by a continuous measurement of the system. The Lindblad evolution (2.7) is obtained from this quantum jump process by averaging over all measurement outcomes. In Section 2.2 we briefly discuss methods for systems with arbitrary coupling strength.

2.1 Quantum Jumps

The open dynamics of a weakly coupled system have an alternative description to the Lindblad equation (2.7) in terms of stochastic differential equations for the wave function of the system. The stochastic dynamics are called unravellings and the average over all trajectories reproduces the Lindblad evolution. The unravellings are not unique. Multiple stochastic descriptions can generate the same Lindblad dynamics, see e.g. [32].

The unravellings can be divided into two main groups. The first group contains quantum jump equations, in which the continuous evolution of the system is interrupted due to random jumps [33, 34, 35, 36]. The second group is quantum state diffusion, where diffusive terms continuously disturb the evolution of the system [37]. The authors of [38, 39] derived the quantum jump equation from a microscopic model and showed how in the limit of small jumps, quantum state diffusion is obtained. Textbook references to unravelling include [25, 40, 41]. Unravelling schemes have also been developed outside the range Lindblad dynamics. Examples of non-Lindblad unravellings are [42, 43]. In this section we focus on quantum jump equations and how they can be understood in terms of generalised measurements.

A generalised measurement in quantum mechanics is an extension to projective measurements. It is described by a set of operators M_α, which describe the effect of a measurement outcome α on the system being measured. The M_α's do not have to be projectors. The operators M_α satisfy the relation

$$\sum_\alpha M_\alpha^\dagger M_\alpha = \mathbb{I}. \tag{2.8}$$

The probability of measuring α, given that the system has the state ρ, is

$$p_\alpha = tr(M_\alpha \rho M_\alpha^\dagger). \tag{2.9}$$

The condition (2.8) guarantees that the outcome probabilities are normalised: $\sum_\alpha p_\alpha = 1$. After a measurement with outcome α, the system is in the state

$$\rho_\alpha = \frac{M_\alpha \rho M_\alpha^\dagger}{tr(M_\alpha \rho M_\alpha^\dagger)}, \tag{2.10}$$

or equivalently if the system has the state vector ψ,

$$\psi_\alpha = \frac{M_\alpha \psi}{\|M_\alpha \psi\|}. \tag{2.11}$$

Note that generalised measurements do not go beyond the standard postulates of quantum mechanics. They can still be described in terms of projective measurements by enlarging the Hilbert space, see e.g. [44].

Let us now consider a specific example of a qubit being continuously measured by a photon detector. At a random time the qubit can emit a photon and when it is absorbed by the detector, we know that the system is in the ground state. The measurement thus has two outcomes: $\alpha = 0$ telling us that no photon has been detected and $\alpha = 1$ meaning that a photon has been detected. We suppose that M_0 is of the form

$$M_0 = \mathbb{I} - iHdt - \frac{1}{2}A^\dagger A dt, \tag{2.12}$$

where $H = H^\dagger$, which leads to

$$M_0^\dagger M_0 = 1 - A^\dagger A dt + O(dt^2). \tag{2.13}$$

From the normalisation condition (2.8), we infer that

$$M_1 = A\sqrt{dt}, \tag{2.14}$$

such that the operators are normalised within $O(dt^2)$ accuracy. We take $A = \sigma_-$ to be the lowering operator of the qubit, since measuring a photon means that the qubit has decayed.

We model the dynamics of the qubit under constant measurement in terms of the increment of the wave function $d\psi(t) = \psi(t + dt) - \psi(t)$. The increment satisfies

$$d\psi(t) = (1 - dN_t)\left(\frac{M_0\psi}{\|M_0\psi\|} - \psi\right)dt + \left(\frac{M_1\psi}{\|M_1\psi\|} - \psi\right)dN_t, \tag{2.15}$$

where dN_t is the increment of a Poisson process, $dN_t = 1$ when the qubit decays and a photon is detected and $dN_t = 0$ otherwise. Let us define $\mathsf{E}(\,.\,)$ to be the average over all realisations of the stochastic process (2.15). Conditioning the average E that the state of the system is ψ at time t, the Poisson increment satisfies

$$\mathsf{E}(dN_t|\psi) = \|M_1\psi\|^2 = \|\sigma_-\psi\|^2 dt. \tag{2.16}$$

The stochastic rules of calculus tell us that the increments dt and dN_t satisfy the product relations [45]

$$\begin{array}{c|cc} \times & dt & dN_s \\ \hline dt & 0 & 0 \\ dN_t & 0 & \delta_{s,t}\, dN_t \end{array}. \tag{2.17}$$

Using the product relations and expanding up to first order in dt, equation (2.15) becomes

$$d\psi(t) = -\left(iH + \frac{\sigma_+\sigma_-}{2} - \frac{\|\sigma_-\|^2}{2}\right)\psi\, dt + \left(\frac{\sigma_-\psi}{\|\sigma_-\psi\|} - \psi\right) dN_t \tag{2.18}$$

Now imagine that the qubit is interacting with the measurement device, but the measurements are not being recorded. We have no information about the current state of the system and only have access to the expected state of the system which is given by

$$\rho(t) = \mathsf{E}(\psi\psi^\dagger). \tag{2.19}$$

Taking the increment of the above equation, one can check that the expected state of the system satisfies

$$\frac{d}{dt}\rho(t) = -i[H, \rho(t)] + \left(\sigma_-\rho(t)\sigma_+ - \frac{1}{2}\{\sigma^+\sigma^-, \rho(t)\}\right), \tag{2.20}$$

which is of the Lindblad form (2.7).

2.2 Strong System-Environment Coupling

While in the case of weak system-bath coupling a method exists to obtain the Lindblad form (2.7), for arbitrary coupling there is no such method. In fact, in general one should not even expect a Lindblad form to accurately describe the dynamics. As the system-bath coupling strength increases, memory effects start to play a role in the evolution of the system. The effective dynamics of the system will depend on its history, which breaks the necessary Markovianity

condition [46, 47]. In practice, when dealing with non-trivially coupled systems, one either has to resort to alternate approximation schemes or numerical methods such as the stochastic Liouville equation [42] or methods based on the phase-space representation, see e.g. [48, 49].

An alternative starting point for both numerical approaches and perturbative expansions are Feynman-Vernon [50, 51] or coherent state [52] path integrals, see e.g. [53, 54, 55]. These path integral formulations resemble the Lagrange formalism to describe classical mechanics where the physical evolution of a system is obtained by considering all paths starting from the initial data. The action functional S gives a weight to each path and the physical evolution is obtained by finding a stationary path of the action. In contrast, in the quantum mechanical path integral approach one sums over the contributions from all paths weighted by the exponential factor e^{iS}.

2.2.1 Non-interacting systems

The class of linear or non-interacting systems are systems whose evolution is described by a Hamiltonian H quadratic in fermionic or bosonic ladder operators

$$H = \sum_{i,j} (\alpha_{ij} a_i^\dagger a_j^\dagger + \beta_{ij} a_i^\dagger a_j + \bar{\alpha}_{ij} a_j a_i), \quad \beta_{ij} \in \mathbb{R}. \tag{2.21}$$

The action functional S describing such Hamiltonians is quadratic in the paths, which means that the weight factor e^{iS} acts as a Fresnel measure, i.e. non-absolutely continuous Gaussian measure for the path integrals. Therefore the dynamics of this system can be integrated exactly. In Chapter 6 we consider such a non-interacting fermion model.

2.2.2 Spin-Boson model

In Article IV the generating function for the heat flowing through a qubit strongly coupled to a hot and a cold bath is studied. The Hamiltonian of the system is

$$H = H_S + H_C + H_H + H_{CS} + H_{HS}. \tag{2.22}$$

The qubit Hamiltonian is given by

$$H_S = -\frac{\Delta}{2}\sigma_x + \frac{\epsilon}{2}\sigma_z. \tag{2.23}$$

The cold bath and hot bath Hamiltonians are

$$H_C = \sum_{n\in C} \omega_n b_n^\dagger b_n, \tag{2.24a}$$

$$H_H = \sum_{n\in H} \omega_n b_n^\dagger b_n. \tag{2.24b}$$

Finally, the system-bath interactions are of the spin-boson type [56]

$$H_{CS} = -\sigma_z \sum_{n\in C} C_n (b_n^\dagger + b_n), \tag{2.25a}$$

$$H_{HS} = -\sigma_z \sum_{n\in H} C_n (b_n^\dagger + b_n). \tag{2.25b}$$

The generating function of the heat flowing to the hot and the cold bath is defined as

$$G_{i,f}(\alpha_C, \alpha_H, t) = \mathrm{tr}_{H,C}\Big(\langle f| e^{i(\alpha_H H_H + \alpha_C H_C)/\hbar} \times U_t e^{-i(\alpha_H H_H + \alpha_C H_C)/\hbar} \Big(\rho_{\beta_C} \otimes \rho_{\beta_H} \otimes |i\rangle\langle i| \Big) U_t^\dagger |f\rangle \Big). \tag{2.26}$$

The above expression cannot be evaluated exactly. In Article IV we apply the Non-Interacting Blip Approximation (NIBA) to obtain an explicit expression for the generating function. The NIBA was originally formulated in terms of the spin-boson path integral [57, 56] and relies on assuming that only certain spin correlation functions are non-zero. The approximation is valid when (a) $\epsilon = 0$ in equation (2.23) (b) for strong coupling and/or high temperatures [58]. x The authors of [59, 60] found that the NIBA is equivalent to the Born-Markov approximation. This can be shown by first applying the polaron transform $U = e^{\sigma_z \Omega}$, with

$$\Omega = \sum_{n\in H,\, C} (C_n/\omega_n)(b_n^\dagger - b_n) \tag{2.27}$$

to the Hamiltonian H. For the transformed Hamiltonian $H' = U^\dagger H U$ we can construct the Redfield equation. Applying the Born-Markov approximation to the Redfield equation gives the same dynamics as those obtained by performing the NIBA. In Article IV we perform the NIBA on the generating function (2.26) via the path integral formulation and as such recover earlier obtained expressions derived with the polaron transform [16, 17].

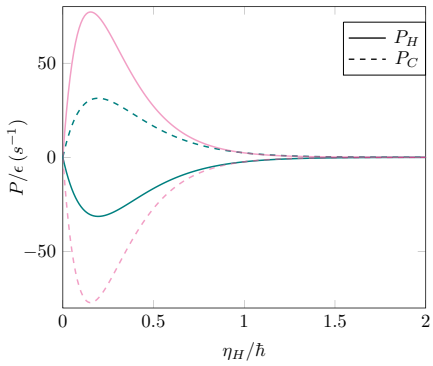

Figure 2.1: The steady state heat current to the cold bath P_C and to the hot bath P_H in function of qubit-hot bath coupling η_H. The purple lines are for the temperature of the hot bath $T_H = 0.2\,\mathrm{K}$ and of the cold bath $T_C = 0.1\,\mathrm{K}$ and the blue lines for the reversed situation $T_H = 0.1\,\mathrm{K}$, $T_C = 0.2\,\mathrm{K}$. The coupling to the cold bath is $\eta_C = 1$. Source: Article IV.

The generating function (2.26) satisfies the Gallavotti-Cohen symmetry [61, 62, 63, 64], which expresses the time-reversal invariance of the microscopic dynamics

$$G_{if}(i\beta_H - \alpha_H/\hbar, i\beta_C - \alpha_C/\hbar, t) = G^R_{fi}(\alpha_H, \alpha_C, t), \tag{2.28}$$

where G^R is the time reversed generating function

$$\begin{aligned} G^R_{i,f}(\alpha_C, \alpha_H, t) = \mathrm{tr}_{H,C}\Big(&\langle i|e^{i(\alpha_H H_H + \alpha_C H_C)/\hbar} \\ &\times U_t^\dagger e^{-i(\alpha_H H_H + \alpha_C H_C)/\hbar}\Big(\rho_{\beta_C} \otimes \rho_{\beta_H} \otimes |f\rangle\langle f|\Big) U_t|i\rangle\Big). \end{aligned} \tag{2.29}$$

This relation still holds after performing the NIBA [16, 17]. In Article IV we derive the implied fluctuation relation. We find that when the both baths are at equal temperature, the variance of the energy exchanged with one of the baths $\mathrm{Var}[\Delta E]$ satisfies

$$\lim_{t\to\infty} \frac{1}{t}\mathrm{Var}[\Delta E] = 2\kappa, \tag{2.30}$$

with κ the thermal conductivity.

Figure 2.1 shows the first moments of the generating function after the NIBA. P_H is the heat flowing to the hot bath and to the cold P_C as a function of η_H,

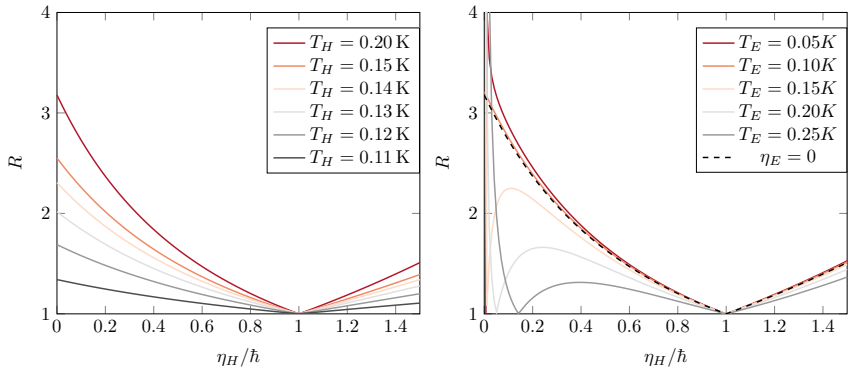

Figure 2.2: (Left) The rectification index (2.31) in the case of two baths, for different temperatures of the hot bath and $T_C = 0.1$K. (Right) The influence of a third bath on the rectification index $T_C = 0.1$K and $T_H = 0.2$K. Source: Article IV.

which represents the coupling between the qubit and the hot bath. Note that when the temperatures of the baths are reversed, the heat current changes sign but the size does not remain the same, except when $\eta_H = \eta_C$ such that the system is symmetric. This phenomenon is called rectification. Figure 2.2 shows the behaviour of the rectification for different temperatures and the influence of a third bath. The rectification index is defined as

$$R = \frac{\max(|P_C|, |P_C^R|)}{\min(|P_C|, |P_C^R|)}, \tag{2.31}$$

where P_C is the power to the cold bath and when the temperatures are exchanged, we define P_C^R as the power to the cold bath, which in this case has a higher temperature than the hot bath.

Chapter 3

Floquet Theory for Quantum Systems

The evolution of a system with a time-periodic Hamiltonian can be expressed in terms of an effective Hamiltonian [11, 65]. This effective description of the motion is a consequence of Floquet's theory for linear periodic partial differential equations [66]. The effective Hamiltonian is therefore often referred to as the Floquet Hamiltonian, and the corresponding driven system as a Floquet system.

The effective Hamiltonian can have drastically different properties than the original non-driven Hamiltonian. A famous example in classical physics is the Kapitza pendulum [67, 68]: by oscillating the base of the pendulum with a high frequency, the vertical-up position of the pendulum can become stable. The possibility of changing a system's properties by applying a periodic driving force leads to a multitude of applications. Using the right properties, it is possible to create systems that show many body localization, have non-trivial topological properties [69] or to construct discrete time crystals [70].

In the context of open quantum systems, Floquet theory is interesting since in the right physical regime, the environment interacts with the effective Hamiltonian rather than with the original Hamiltonian of the system. The corresponding Lindblad equation induces transitions between the effective eigenstates instead of the energy eigenstates of the system as usual.

In the next section, we will briefly introduce Floquet theory for closed quantum systems and discuss the equivalence of the Floquet Hamiltonian with a fully second quantised model. Floquet theory for weakly coupled open systems is discussed in Section 3.2, including the contribution of Article I.

3.1 Floquet theory for Closed Quantum Systems

The Schrödinger equation for a time dependent Hamiltonian and initial condition ψ_0 for the wave function is

$$\begin{cases} (H(t) - i\hbar\partial_t)\psi(t) = 0 \\ \psi(0) = \psi_0. \end{cases} \tag{3.1}$$

In case of periodic time dependence of the Hamiltonian $H(t+T) = H(t)$, Floquet's theorem tells us that the unitary time evolution operator $U(t)$ has the structure

$$U(t) = P_{t,0}e^{-iDt}, \tag{3.2}$$

where $P_{t,0}$ is a unitary T-periodic matrix and D is Hermitian [11, 65]. Since D is Hermitian it can be fully diagonalised with real eigenvalues ϵ_i and eigenvectors φ_i that evolve as

$$P_{t,0}e^{-iDt}\varphi_i = e^{-i\epsilon_i t}\phi_i(t), \tag{3.3}$$

where we defined the periodic state

$$\phi_i(t) = P_{t,0}\varphi_i. \tag{3.4}$$

Note that replacing $\phi_i(t)$ by $\phi_{i,n}(t) = e^{i\frac{2\pi n}{T}t}\phi_i(t)$ and ϵ_i by $\epsilon_i + \frac{2\pi n}{T}$ does not change the left hand side of equation (3.3). We have an additional freedom in choosing ϕ_i and ϵ_i, for example to take $\epsilon_i \in]-\frac{2\pi}{2}, \frac{2\pi}{2}]$. The states $\phi_{i,n}(t)$ are called Floquet states and solve the eigenvalue problem

$$\begin{cases} (H(t)\psi(t) - i\hbar\partial_t)\phi_{i,n}(t) = (\epsilon_i + \frac{2\pi n}{T})\phi_{i,n}(t) \\ \phi_{i,n}(t+T) = \phi_{i,n}(t). \end{cases} \tag{3.5}$$

The above set of equations is an eigenvalue problem in the Hilbert space $\mathbb{H} \otimes L^2[0,T]$ with $\mathbb{H}$ the original Hilbert space of the system. The scalar product $\langle\,.\,|\,.\,\rangle$ in $\mathbb{H}$ is extended by

$$\langle f, g\rangle_{L^2} = \frac{1}{T}\int_0^T d\tau \langle f(\tau)|g(\tau)\rangle. \tag{3.6}$$

In this Hilbert space, the Floquet states $\phi_{i,n}$ form an orthonormal basis.

The action of $P_{t,0}$ on ψ_0 can be expressed in terms of the Floquet states

$$P_{t,0}\psi = \sum_i \phi_i(t)\langle\varphi_i|\psi\rangle \tag{3.7}$$

such that $\psi(t)$ evolved from an initial state $\psi_0 \in \mathbb{H}$ can be written as

$$\begin{aligned}\psi(t) &= \sum_i e^{-i\epsilon_i t}\phi_i(t)\langle\varphi_i|\psi_0\rangle \\ &= \sum_n \sum_i e^{-i(\epsilon_i + 2\pi n/T)t}\phi_{i,n}(t)\frac{1}{T}\int_0^T d\tau\, e^{i(2\pi n/T)\tau}\,\langle\varphi_i|\psi_0\rangle. \end{aligned} \tag{3.8}$$

By inserting the identity $\mathbb{I} = P^\dagger_{\tau,0}P_{\tau,0}$ in the integral we arrive at

$$\psi(t) = \sum_n \sum_i e^{-i(\epsilon_i + 2\pi n/T)t}\phi_{i,n}(t)\frac{1}{T}\int_0^T d\tau\,\langle\phi_{i,n}(\tau)|P_{\tau,0}\psi\rangle. \tag{3.9}$$

The above equation may look like a unnecessary convoluted expression for $\psi(t)$. However, it will help us relate the dynamics in $\mathbb{H}$ governed by $H(t)$ to the dynamics of the system in the Hilbert space $\mathbb{H}\otimes L^2[0,T]$ with Hamiltonian

$$H_F(\tau) = H(\tau) - i\partial_\tau. \tag{3.10}$$

Note that τ does not represent time but the periodic spatial coordinate of $L^2[0,T]$. An initial state $\Psi_0 \in \mathbb{H}\otimes L^2[0,T]$ evolves as

$$\Psi(\tau,t) = \sum_n \sum_i e^{-i(\epsilon_i + 2\pi n/T)t}\phi_{i,n}(\tau)\frac{1}{T}\int_0^T d\tau\,\langle\phi_{i,n}(\tau)|\Psi_0(\tau)\rangle. \tag{3.11}$$

By comparing equations (3.9) and (3.11), we find that the state $\psi(t) \in \mathbb{H}$ can be lifted to the larger Hilbert space with the relation

$$\Psi(\tau,t) = P_{\tau,t}\psi(t), \tag{3.12}$$

and initial condition $\Psi(\tau,0) = P_{\tau,0}\psi_0$. The above relation tells us that both systems are related by lifting the T-periodic time dependence of $\psi(t)$ to a periodic spatial coordinate. Equation (3.12) implies $\psi(t) = \Psi(\tau,t)|_{\tau=t}$ [13, 14].

The expanded Hilbert space has the advantage that it can be related to a physical system. Already in 1965 [11], Shirley noted the equivalence between a periodically driven system and a fully second quantized description of the system interacting with a harmonic oscillator. The oscillator has frequency $\omega_L = 2\pi/T$. In the limit that the average excitation number of the oscillator goes to infinity, the Floquet states $\phi_{i,n}(t)$ correspond to energy eigenstates of the qubit-oscillator with energies $\epsilon_i + \hbar\omega_L$. The term $\frac{-i}{\omega_L}\partial_\tau$ can be interpreted as the number operator for the oscillator and therefore factors $e^{in\omega_L\tau}$ increase the expected photon number by n. The authors of [12] made this equivalence rigorous for a concrete Hamiltonian.

3.2 Floquet Description for Strongly Driven Open Systems

The description of driven systems in contact with an environment is a non-trivial matter, even in case system and environment are weakly coupled. When considering arbitrarily strong and fast driving, necessary assumptions needed to justify the weak-coupling limit can break down. Generally, there are two cases for which the usual Lindblad equation can be used. Firstly, when the strength of the driving is of the order of the system-bath coupling squared, i.e. weak driving. Secondly, when the driving is much slower than the characteristic time scale of system-bath interactions, i.e. adiabatic driving.

When the driving is strong and fast enough, the environment effectively interacts with the time averaged system. The weak coupling limit can be performed by expressing the system-bath interaction in terms of eigenoperators of the Floquet Hamiltonian [71]. The interaction with the bath leads to transitions between Floquet states instead of the energy eigenstates of the system. We call the resulting master equation for the system the Floquet-Lindblad equation.

One of the assumptions made by [71] is that the inverse of the difference of the Floquet quasi-energies is much smaller than the characteristic timescale τ_R of the system-bath interactions

$$|\epsilon_r - \epsilon_s + k\frac{2\pi}{T}|^{-1} \ll \tau_R \quad \text{for } k \in \mathbb{Z}. \tag{3.13}$$

This assumption is needed to perform the so-called rotating wave approximation. In some cases the differences $|\epsilon_r - \epsilon_s|$ can be very small. If so, one can make a partial rotating wave approximation [72, 73, 74, 75, 76], which leads to additional terms in the resulting Floquet-Lindblad equation. In this section, and in Article I and II, we maintain assumption (3.13) and perform the full rotating wave approximation. Furthermore, we assume that there are no degeneracies in the Floquet energy spectrum

$$\epsilon_r \neq \epsilon_{r'} + k'\frac{2\pi}{T} \quad \text{for } r \neq r',\ k \in \mathbb{Z}. \tag{3.14}$$

Let us now consider a periodically driven system as in the last section, which interacts with a bath through the interaction Hamiltonian

$$H_I = X \otimes \sum_k (B_k + B_k^\dagger), \tag{3.15}$$

where X is the interaction coordinate of the system and B_k are bath operators.

The Floquet-Lindblad operators A are calculated by transforming the interaction coordinate X to the interaction picture. The resulting expression can be cast into the form

$$U^\dagger(t,t_0)XU(t,t_0) = \sum_{\omega\in\Omega} A(\omega,t_0)e^{-i\omega(t-t_0)} \tag{3.16}$$

where the summation is over the set

$$\Omega = \{\epsilon_i - \epsilon_j + n\frac{2\pi}{T} | n \in \mathbb{Z}\}. \tag{3.17}$$

The operators $A(\omega,t)$ are eigenoperators of the Floquet Hamiltonian $H_F(t)$: they satisfy

$$[H(t) - i\partial_t, A(\omega,t)] = -\omega A(\omega,t). \tag{3.18}$$

Assumption (3.14) assures that $A(\omega,t)$ projects a Floquet state $\phi_r(t)$ on a unique Floquet state $\phi_{s_r}(t)$

$$A(\omega,t)\phi_r(t) = \alpha_{r,\omega}e^{in_{r,\omega}\frac{2\pi}{T}t}\phi_{s_{r,\omega}}(t), \tag{3.19}$$

where $s_{r,\omega}$ and $n_{r,\omega}$ are unique such that

$$\epsilon_r - \epsilon_{s_{r,\omega}} - n_{r,\omega}\frac{2\pi}{T} = \omega \tag{3.20}$$

and $\alpha_{r,\omega} \in \mathbb{C}$. The Floquet-Linblad equation is

$$\begin{aligned}\frac{d}{dt}\rho(t) =& -i[H(t),\rho(t)] \\ &+ \sum_\omega \gamma(\omega)(A(\omega,t)\rho(t)A^\dagger(\omega,t) - \frac{1}{2}\{A^\dagger(\omega,t)A(\omega,t),\rho(t)\}),\end{aligned} \tag{3.21}$$

where the $\gamma(\omega)$'s are the transition rates. Similar to the jump process discussed in Section 2.1, the above Lindblad equation can be unravelled as [77]

$$d\psi(t) = -iG(\psi(t))dt + \sum_{\omega\in\Omega}\left(\frac{A(\omega,t)\psi(t)}{\|A(\omega,t)\psi(t)\|} - \psi(t)\right)dN(\omega,t) \tag{3.22}$$

with

$$G(\psi) = -i\frac{1}{2}\sum_{\omega\in\Omega}\gamma(\omega)(A^\dagger(\omega,t)A(\omega,t) - \|A(\omega,t)\psi(t)\|^2)\psi(t) \tag{3.23}$$

and

$$\mathsf{E}(dN(\omega,t)|\psi) = \gamma(\omega)\|A(\omega,t)\psi\|^2 dt. \tag{3.24}$$

From equation (3.21) it is straightforward to check that the diagonal elements of the density matrix in the Floquet basis satisfy a closed equation. Let us define $P_r(t)$ as the probability to be in the Floquet state $\phi_r(t)$ at time t

$$P_r(t) = \langle\phi_r(t)|\rho(t)|\phi_r(t)\rangle. \tag{3.25}$$

Projecting on $\phi_r(t)$ on both sides of equation (3.21), we find that the probabilities satisfy a Pauli master equation

$$\frac{d}{dt}P_r(t) = \sum_s [W(r|s)P(s) - W(s|r)P(r)] \tag{3.26}$$

with the transition rates

$$W(s|r) = \sum_\omega \gamma(\omega)|\alpha_{r,\omega}|^2 \delta_{s_{r,\omega},r}. \tag{3.27}$$

3.2.1 Equivalence

In Article I the relation (3.12), connecting the $\mathbb{H}$ and $\mathbb{H}\otimes L^2$ system, is extended to open systems. We consider the Floquet system with Hamiltonian $H_F(\tau)$ in the Hilbert space $\mathbb{H}\otimes L^2[0,T]$ to be in contact with a bath with the interaction Hamiltonian

$$\tilde{H}_I = X \otimes \mathbb{I}_{L^2} \otimes \sum_k (B_k + B_k^\dagger) \tag{3.28}$$

where X is the same system interaction coordinate as in (3.15) and $\mathbb{I}_{L^2}$, the identity operator in L^2. Under the weak coupling limit, one can derive a stochastic Schrödinger equation for this system.

Let us now assume that there exists a unique $n_\omega \in \mathbb{Z}$ for all transition frequencies $\omega \in \Omega$, see equation (3.17), such that

$$\omega = \text{difference of quasi-energies } + n_\omega \frac{2\pi}{T}. \tag{3.29}$$

Note that in the case the driven system is a qubit, this assumption is equivalent to (3.14). Thus, n_ω is the amount of particles annihilated, or created for $n_\omega < 0$, in the driving field during the transition $A(\omega)$. We introduce the process $\mu(t)$,

which counts the change in photon number during the evolution of the system. The counting process evolves as

$$d\mu(t) = \sum_{\omega\in\Omega} n_\omega dN(\omega). \tag{3.30}$$

In Article I, we find that by simultaneously evolving the set of equations

$$\begin{cases} d\psi(t) = -iG(\psi(t))dt + \sum_{\omega\in\Omega}\left(\frac{A(\omega,t_0)\psi(t)}{\|A(\omega,t_0)\psi(t)\|} - \psi(t)\right) dN(\omega) \\ d\mu(t) = \sum_{\omega\in\Omega} n_\omega dN(\omega) \end{cases} \tag{3.31}$$

and defining the state in the larger Hilbert space $\mathbb{H}\otimes L^2$

$$\Psi(t,\tau) = e^{-i\mu(t)\omega_L\tau} P_{\tau,t_0}\psi(t), \tag{3.32}$$

the state $\Psi(t,\tau)$ evolves according to the stochastic Schrödinger for the $\mathbb{H}\otimes L^2[0,T]$ system. Figure 3.1 illustrates relation (3.32) for a driven two level system.

Using the relation (3.32) between both systems, the thermodynamics of a periodically driven qubit are studied through the $\mathbb{C}^2\otimes L^2$ system in Article I. In this way, earlier results obtained by [78, 79] are recovered.

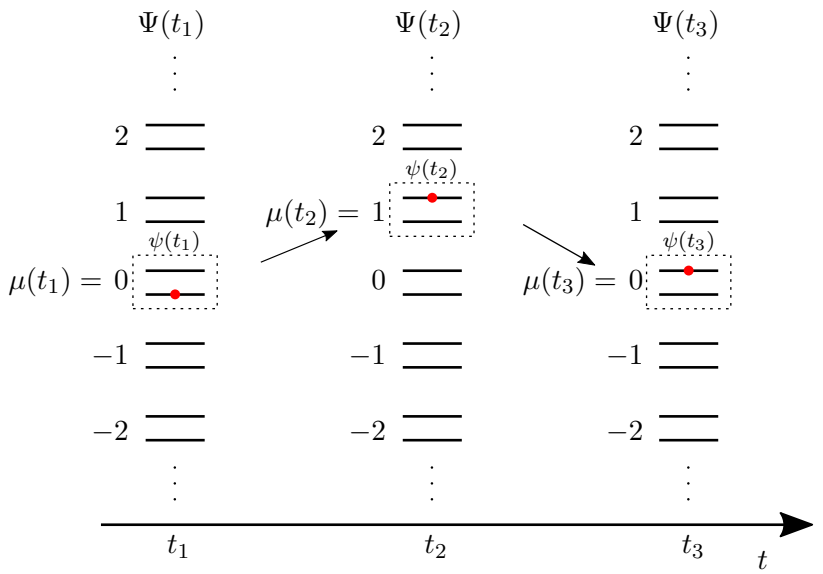

Figure 3.1: A visualisation of the stochastic process given by the couple of equations (3.31) and the relation (3.32) with jumps at times t_1, t_2, ... The qubit state is initialised in the lower Floquet state ϕ_- and initially no photons have been created or annihilated in the drive, so $\mu(t_0) = 0$. Source: Article I.

Chapter 4

Calorimetric Measurements

The authors of [18] proposed an experimental setup to perform calorimetric measurements of the heat exchange between a qubit and its environment. The idea is to measure temperature changes in the environment induced by energy exchanges with the qubit. Concretely, the setup they propose is based upon a quantum integrated circuit containing a superconducting qubit and a resistor, which acts as the calorimeter. Figure 4.1 shows a visual representation of the quantum integrated circuit.

The experiment [18] requires the realization of a nanoscale thermometer to measure the temperature of the resistor. The possibility to actually construct such devices was proven in [19] with a thermometer based on an NIS junction, recent realisations include [80, 81]. The working principle of this thermometer is that the conductance of the junction depends on the temperature of the normal metal and is independent of the superconductor temperature. By applying a small bias current through the junction, one can extract the temperature while minimally disturbing the system. Improvements to the design and resolution of the thermometer have been made by [20, 21, 82].

The proposal by [18] and general possibility of calorimetric measurements in quantum integrated circuits motivated several theoretical studies into systems interacting with a finite environment [83, 84, 85, 86, 22, 87]. In [83] the authors studied the statistics of work by counting photons absorbed and emitted from the environment using the quantum jump approach. The authors of [85] proposed a simultaneous jump process for a system and the energy of the environment. In [86], the authors derived the master equation corresponding to the the system-energy jump process of [85]. Such a master equation describing the simultaneous evolution of a classical and quantum variable is usually referred to as a hybrid

master equation. The authors of [22] proposed a similar jump process to [85], but related energy exchanges to changes in the temperature environment. By treating the electrons in the calorimeter as free particles, the Sommerfeld expansion [88] relates changes of the calorimeter energy dE to changes in its temperature (squared) dT_e^2.

$$dT_e^2 = \frac{1}{N\sigma} dE, \tag{4.1}$$

where N is the amount of electrons in the calorimeter and σ a constant. From this relation it is clear that the change in temperature goes to zero as the size of the calorimeter goes to infinity, and hence the amount of electrons $N \to \infty$. Furthermore, the authors of [22] considered the influence of the substrate on which the integrated circuit is placed in experiments such as [18]. The electrons and phonons in the resistor exchange energy, while phonons in the substrate keep the resistor phonons at a constant temperature. This interaction leads to an additional drift term for dE [89, 90]

$$dE_{ep} = \Sigma V (T_p^5 - T_e^5) dt, \tag{4.2}$$

which drives the electron temperature T_e to the phonon temperature T_p. Σ is a material constant and V the volume of the calorimeter. The temperature drift (4.2) caused by the electron-phonon interaction is a typical occurrence in integrated circuits [91]. For example, the recent study [92] investigates the drift term and observes a crossover to the power law $dE_{ep} \propto T_p^4 - T_e^4$ as the electron-phonon energy transfer comes to dominate phonon-substrate phonon energy transfer. Fluctuations in the electron-phonon energy exchange lead to an additional noise term for dE [93]

$$dE_{\text{noise}} = \sqrt{10\Sigma V} T_p^3 dw_t. \tag{4.3}$$

Recently, the authors of [87] studied a system-environment jump process similar to [22] by including the response of the thermometer measuring the calorimeter, smearing out the measured jumps.

In Articles II & III we study the qubit-calorimeter setup for a periodically driven qubit. In Article III we model the dynamics of the qubit-calorimeter state $\rho(X, t)$, where $X = T_e^2$, with the hybrid master equation corresponding to the

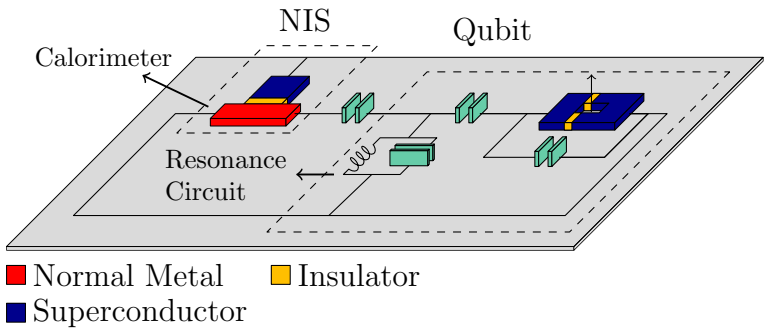

Figure 4.1: Experimental setup proposed by [18].

jump process [22]

$$\begin{aligned}\frac{d\rho}{dt}(X,t) &= \mathcal{L}_X\rho(X,t) - i[\hbar\omega_0\sigma_z + \kappa H(t), \rho(X,t)] \\ &+ \left(\Gamma_\downarrow\left(X - \frac{\hbar\omega_0}{N\sigma}\right)\sigma_-\rho\left(X - \frac{\hbar\omega_0}{N\sigma}\right)\sigma_+ - \frac{\Gamma_\downarrow(X)}{2}\{\sigma_+\sigma_-, \rho(X,t)\}\right) \\ &+ \left(\Gamma_\uparrow\left(X + \frac{\hbar\omega_0}{N\sigma}\right)\sigma_+\rho\left(X + \frac{\hbar\omega_0}{N\sigma}\right)\sigma_- - \frac{\Gamma_\downarrow(X)}{2}\{\sigma_-\sigma_+, \rho(X,t)\}\right). \quad (4.4)\end{aligned}$$

The second and third line in the above equation have a form similar to the dissipator terms in the Lindblad equation (2.7). They are due to the qubit-calorimeter interaction. The drift (4.2) and diffusion (4.3) due to the electron-phonon interaction are contained in in the operator

$$\mathcal{L}_X f(X,t) = -\frac{\Sigma V}{N\sigma}\partial_X[(T_p^5 - X^{2/5})f(X,t)] + \frac{10\Sigma V k_B T_P^6}{2N^2\sigma^2}\partial_X^2 f(X,t). \quad (4.5)$$

One of the underlying assumptions for equation (4.4) is that the driving strength κ is of the order of the qubit-calorimeter coupling strength, such that the driving is a perturbation to the free evolution of the qubit. Hence, we refer to equation (4.4) as the weak-driving hybrid master equation.

In Article II we use the Floquet formalism for periodically driven open quantum systems presented in Section 3.2 to model the qubit-temperature dynamics. Analogously to the Pauli master equation (3.26), the probability $P(r, X, t)$ for the qubit to be in Floquet state r and the calorimeter to have temperature square

$X = T_e^2$ at time t satisfies a classical equation

$$\frac{dP}{dt}(r, X, t) = \mathcal{L}_X P(r, X, t) + \sum_s \int_0^\infty dY\, W(r, X|s, Y) P(s, Y, t) - \sum_s \int_0^\infty dY\, W(s, Y|r, X) P(r, X, t) \tag{4.6}$$

with the qubit-temperature transition rates

$$W(r, X|s, Y) = \sum_\omega \Gamma(\omega, Y) |\alpha_{r,\omega}|^2 \delta_{s_{r,\omega},s} \delta\left(X - Y - \frac{\hbar\omega}{N\sigma}\right). \tag{4.7}$$

4.1 Numerical Predictions

The weak-driving master equation (4.4) and the Floquet jump process (4.6) both provide descriptions of the qubit-calorimeter dynamics. The underlying assumptions for both equations do not necessarily match: equation (4.4) requires the driving to be much weaker than the free evolution of the qubit while (4.6) requires the driving to be much stronger than the interaction with the calorimeter. By numerically integrating the dynamics of both equations, we can provide quantitative predictions for the experiment [18]. Additionally, we are able to compare the predictions made by the two different approximative schemes in terms of a measurable quantity, the temperature of the calorimeter. In Article II we integrate the dynamics of the Floquet jump equation (4.6). In Article III we compare the predictions of equations (4.4) and (4.6).

In the upcoming numerics we study the behaviour of the temperature for different values of the qubit-calorimeter coupling and the driving strength. The coupling strength is represented by the dimensionless quantity g^2 and the driving strength by κ. The drive is taken to be

$$H(t) = e^{-i\omega_0 t}\sigma_+ + e^{i\omega_0 t}\sigma_+. \tag{4.8}$$

For our specific model, assumption (3.13) for the Floquet-Lindblad equation requires that [25]

$$\frac{g^2}{\kappa} \ll 1. \tag{4.9}$$

Figure 4.2 shows the distribution of the temperature after 10 periods of driving. Note that equations (4.4) and (4.6) predict similar behaviour even when g^2 is of the same order as κ. When $g^2 > \kappa$ the predictions are significantly different.

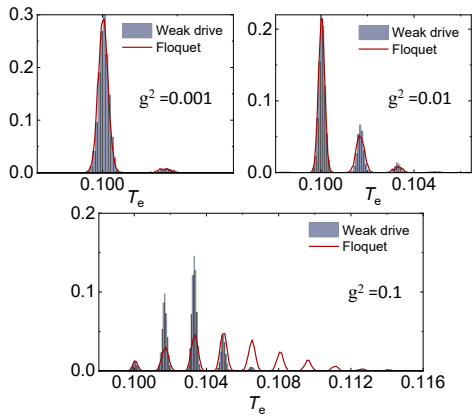

Figure 4.2: Distribution of the electron temperature T driving for $10\times 2\pi/\omega$ for $\kappa = 0.05$. The red line displays the temperature distribution predicted by the Floquet master equation (4.6), the (blue) histogram comes from the weak drive dynamics (4.4). The physical parameters used in the numerical integration are $\hbar\omega = 0.5k_B \times 1$ K, is $V = 10^{-21}\mathrm{m}^3$, $\Sigma = 2 \times 10^{-9}$ W $\mathrm{K}^{-5}\mathrm{m}^{-3}$ and $\gamma = 1500k_B/(1\mathrm{K})$. Source: Article III.

After many driving cycles the temperature increases until the electron-phonon interaction balances out the energy provided from the qubit to the calorimeter. Figure 4.3 illustrates this relaxation to the steady state. While measuring the short time temperature statistics is still an experimental challenge [94, 95], the average temperature in steady state is possible, see for example the recent experiments [80, 81]. Figure 4.4(a) compares predictions of the average steady state temperatures by the weak-driving (4.4) and Floquet (4.6) equations. The dashed lines are the Floquet predictions. For fixed coupling strength g^2 increasing the driving strength κ barely influences the steady state temperature. The dots with error bars represent the weak-driving dynamics. As the driving strength increases, the dots asymptotically reach the Floquet lines.

Finally, in Figure 4.4(b) we show the parametric region in which both predictions overlap. The green area below the black squares represents values for κ and g^2 for which the constant Floquet lines fall within the error bars of the weak-driving results in Figure 4.4(a). The slope between the two regions is 0.454 ± 0.013 indicating that when κ is about twice as large as g^2, both systems predict the same statistics.

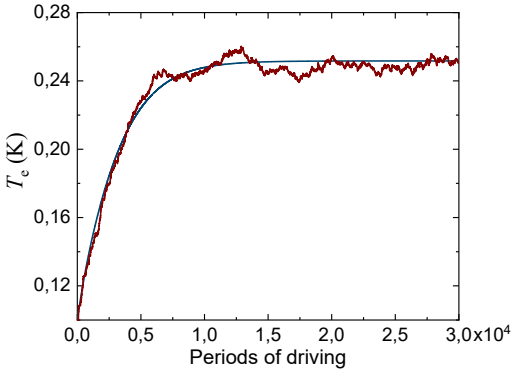

Figure 4.3: After many periods of driving the temperature reaches a steady state, when the energy provided by the driven qubit matches the energy dissipating due to the electron-phonon interaction. Source: Article II.

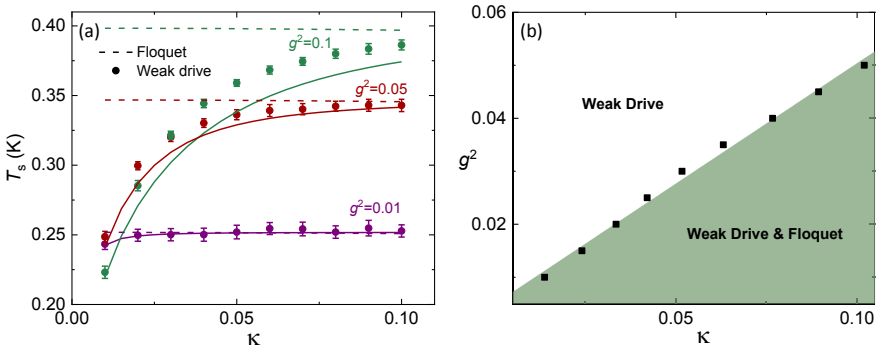

Figure 4.4: (a) Dependence of average steady state temperature on the driving strength κ for coupling contant g. The dashed lines show the steady state temperature predicted by the Floquet jump equation (4.6), the dots show predictions obtained by numerically integrating (4.4) (b) Parametric region for which the Floquet and weak-driving equations predict the same steady state temperature. In the green region below the black squares, the dashed lines in (a) fall within the standard deviation of the dots. The parameters used for the simulations are in the caption of Figure 4.2. Source: Article III

Chapter 5

Multiscale Perturbation theory

The theory of multiscale perturbation provides a technique to construct approximate solutions to differential or partial differential equations. Applying ordinary perturbation theory to such problems can lead to secular terms, i.e. diverging terms. These divergences can be, at least partially, resolved by resuming the expansion. An illustrative example of how secular terms can arise by finite order expansions is to consider the truncated expansion of $e^{-\varepsilon t}$ [96]

$$1 - \varepsilon t + \frac{1}{2}\varepsilon^2 t^2 + \ldots + (-1)^n \frac{1}{n!}\varepsilon^n t^n. \tag{5.1}$$

Clearly all individual terms, except the zeroth order, are diverging for large positive t as well as their finite sum. However, $e^{-\varepsilon t}$ is bounded for all positive t.

Multiscale perturbation theory provides a more refined method of constructing approximate solutions than ordinary perturbation theory. In mathematics literature it is referred to as homogenization [97]. The method relies on identifying different (time) scales in the problem and to treat these scales as independent variables. Doing so, allows one resum secular terms at finite orders in the expansion.

The theory of multiscale perturbations was used multiple times in the articles on which this dissertation is based. In the Article II and Article III the long time behaviour of equations (4.4) and (4.6) is studied analytically, by averaging out the qubit dynamics with a multiscale perturbative expansion. Also in Chapter 6 this technique is used to derive the hybrid master equation in the weak coupling limit. In fact, the rigorous derivation of the Lindblad equation (2.7), can be thought of as a multi-timescale expansion.

In the next section we illustrate the difference between ordinary and multi-timescale perturbation theory with an example. In Section 5.2, we discuss the results obtained in the Article II and Article III.

5.1 Motivating Example

Let us look at an example of a multi-timescale perturbation, see [98] for more details. We consider the differential equation

$$\ddot{x} + 2\varepsilon\dot{x} + x = 0. \tag{5.2}$$

with initial conditions $x(0) = 0$ and $\dot{x}(0) = 1$ and ε gives the strength of the perturbation. For this example, the exact solution is known to be

$$x(t, \varepsilon) = (1 - \varepsilon^2)^{-1/2} e^{-\varepsilon t} \sin\left((1 - \varepsilon^2)^{1/2} t\right). \tag{5.3}$$

It is clear that $x(t, \varepsilon)$ is bounded for all t and $\varepsilon < 1$. From the exact solution, we can immediately detect multiple time scales of the problem. The sine function contains the fastest time t, followed by the exponential decay εt. Even slower time scales are found in the sine function.

5.1.1 Ordinary Perturbation

We start by doing a simple perturbative expansion of the solution in ε: $x(t, \varepsilon) = x_0(t) + \varepsilon x_1(t) + \ldots$. Plugging the expansion in equation (5.2) leads to a set of equations for all orders of ε

$$\begin{cases} \varepsilon^0 : & \ddot{x}_0 + x_0 = 0 \\ \varepsilon^1 : & \ddot{x}_1 + 2x_0 + x_1 = 0 \\ \vdots & \end{cases} \tag{5.4}$$

Solving the 0th order equation is straightforward and gives

$$x_0(t) = \sin t. \tag{5.5}$$

Using the solution of $x_0(t)$ for the first order equation leads to

$$\ddot{x}_1 + x_1 = -2\cos t, \tag{5.6}$$

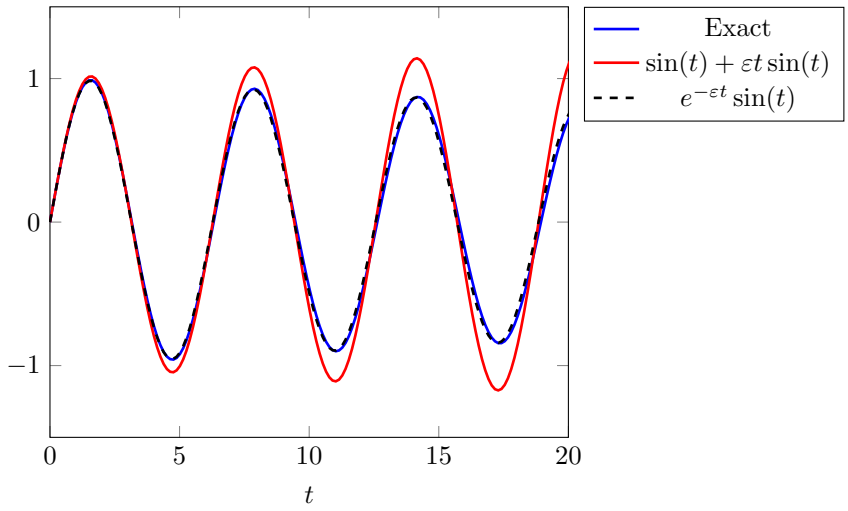

Figure 5.1: A plot comparing the exact solution (5.2) to the solution obtained by ordinary perturbation theory (5.8) and by multiscale perturbation theory (5.15). $\varepsilon = 0.01$.

which has the solution

$$x_1(t) = -t \sin t. \tag{5.7}$$

Up to first order in ε, the solution to (5.2) is

$$x(t, \varepsilon) = \sin t + \varepsilon t \sin t + O(\varepsilon^2). \tag{5.8}$$

Comparing the exact solution (5.3) to the approximate (5.8), one can see that the perturbative solution remains close to the exact one for short times $t\varepsilon \ll 1$. For longer times, however, both solutions predict significantly different qualitative behaviour: (5.3) decays to 0, while (5.8) continues to grow linearly, see also Figure 5.1.

5.1.2 Multiscale perturbation

Let us now take advantage of our knowledge of the different time scales of the exact solution (5.3) and introduce the slow time $\tau = \varepsilon t$. We explicitly write the time dependence of the solution on τ

$$x(t, \varepsilon) \to x(t, \tau, \varepsilon) = x_0(t, \tau) + \varepsilon x_1(t, \tau) + O(\varepsilon^2). \tag{5.9}$$

Accordingly, the time derivative changes to

$$\dot{x}(t) = \frac{d}{dt}x(t) = \partial_t x(t,\tau) + \frac{\partial\tau}{\partial t}\partial_\tau x(t,\tau) = \partial_t x(t,\tau) + \varepsilon\partial_\tau x(t,\tau) \tag{5.10}$$

Combing (5.9) and (5.10) with our original problem (5.2), we find the set of equations for all orders

$$\begin{cases} \varepsilon^0: & \partial_t^2 x_0 + x_0 = 0 \\ \varepsilon^1: & \partial_t^2 x_1 + 2\partial_\tau\partial_t x_0 + 2\partial_t x_0 + x_1 = 0 \\ \vdots & \end{cases} \tag{5.11}$$

Solving the first equation gives

$$x_0(t,\tau) = A(\tau)\sin t + B(\tau)\cos t. \tag{5.12}$$

Note that there is freedom in the τ dependence A and B. Applying the solution of x_0 to the first order equation leads to

$$\partial_t^2 x_1 + x_1 = -2(\partial_\tau A + A)\cos t + 2(\partial_\tau B + B)\sin t \tag{5.13}$$

The right hand side of this equation has the risk of leading to diverging terms just as we saw in the first order term (5.7) for the ordinary perturbation theory. However, since we want to avoid such terms, we impose

$$\partial_\tau A + A = 0 = \partial_\tau B + B \tag{5.14}$$

Combining this condition with the initial conditions $x(0) = 0$ and $\dot{x}(0) = 1$, we find

$$x(t) = e^{-\tau}\sin t + O(\varepsilon) = e^{-\varepsilon t}\sin t + O(\varepsilon) \tag{5.15}$$

Now, comparing to the exact solution (5.3), it is immediately clear that the approximation captures both the oscillations and the exponential decay. Figure 5.1 shows the exact solution and the first order approximation by both types of perturbative expansions.

5.2 Effective Dynamics for the Temperature

In Article II and Article III, the qubit-calorimeter system is described by the master equations (4.6) and (4.4), respectively. One of the goals of the articles is

to study the long time behavior of the temperature of the Calorimeter. To do so it is convenient to eliminate the qubit degrees of freedom and to obtain effective dynamics for the temperature.

The idea of Articles II and III is to expand around an infinite size calorimeter. In this limit the qubit-calorimeter interactions take place on a time scale in which the temperature remains approximately constant. The qubit has time to equilibrate with the calorimeter on its current temperature and only on much longer timescales the temperature changes. The expansion parameter is introduced by scaling the amount of electrons N by ε. Accordingly, we define the time scale $\tau = \varepsilon t$ and furthermore take the limit where the short time dynamics have already relaxed

$$\bar{\rho}(X,\tau) = \lim_{t\to\infty} \rho(X,t,\tau). \tag{5.16}$$

Expanding the hybrid master equation (4.4) in ε leads to

$$\begin{aligned}\varepsilon \frac{d}{d\tau}\bar{\rho}(X,\tau) = &-\varepsilon \frac{\Sigma V}{N\sigma}\partial_X[(T_p^5 - X^{2/5})\bar{\rho}(X,\tau)] + \varepsilon^2 \frac{10\Sigma V k_B T_P^6}{2N^2\sigma^2}\partial_X^2\bar{\rho}(X,\tau) \\ &+ M^{(0)}(\bar{\rho})(X,\tau) + \sum_{n=1}^{\infty}\frac{\varepsilon^n}{n!}M^{(n)}(\bar{\rho})(X,\tau).\end{aligned} \tag{5.17}$$

Let us represent the density matrix in terms of a vector containing its components: $\rho = \begin{pmatrix}\rho_{11} & \rho_{22} & \rho_{12} & \rho_{22}\end{pmatrix}^T$. In the case of the weak-driving dynamics (4.4) with driving (4.8), the matrices M have the form

$$M^{(0)}(X) = \begin{pmatrix} -\Gamma_\downarrow(X) & \Gamma_\uparrow(X) & i\lambda & -i\lambda \\ \Gamma_\downarrow(X) & -\Gamma_\uparrow(X) & -i\lambda & i\lambda \\ i\lambda & -i\lambda & -\Gamma(X)/2 & 0 \\ -i\lambda & i\lambda & 0 & -\Gamma(X)/2 \end{pmatrix}, \tag{5.18}$$

where we defined the sum of the rates

$$\Gamma(X) = \Gamma_\downarrow(X) + \Gamma_\uparrow(X) \tag{5.19}$$

and the higher orders are

$$M^{(n)}(X) = \left(\frac{\hbar\omega}{\gamma}\right)^n \begin{pmatrix} 0 & \Gamma\uparrow(X) & 0 & 0 \\ (-1)^n\Gamma\downarrow(X) & 0 & 0 & 0 \\ 0 & 0 & 0 & 0 \\ 0 & 0 & 0 & 0 \end{pmatrix}. \tag{5.20}$$

Note that $M^{(0)}$ is the matrix representation of the usual Lindblad equation of a qubit interacting with a bath at temperature $\sqrt{X}$ with driving (4.8).

In analogy to the example worked out in the last section, the above perturbative expansion gives a hierarchy of differential equations

$$\begin{cases} \varepsilon^0: & M^{(0)}\rho^{(0)}(X,\tau) = 0 \\ \varepsilon^1: & \partial_\tau \rho^{(0)}(X,\tau) - M^{(0)}\rho^{(1)}(X,\tau) - M^{(1)}\rho^{(0)}(X,\tau) \\ & \qquad + \frac{\Sigma V}{N\sigma}\partial_X[(T_p^5 - X^{2/5})\bar{\rho}(0)(X,\tau)] = 0 \\ \vdots & \end{cases} \tag{5.21}$$

Solving the zeroth order equation, we find

$$\rho^{(0)}(X,\tau) = Q(X)F^{(0)}(X,\tau) \tag{5.22}$$

where $Q(X)$ satisfies $M^{(0)}Q(X) = 0$ and is thus the steady-state solution of the driven system interacting with a bath on temperature $\sqrt{X}$ and $F^{(0)}(X,\tau) = \operatorname{tr}\rho^{(0)}(X,\tau)$.

Solving the qubit dynamics up to second order, we derive an effective Fokker-Planck equation for $F(X,\tau) = F^{(0)}(X,\tau) + \varepsilon \operatorname{tr}\rho^{(1)}(X,\tau)$

$$\begin{aligned} \partial_\tau F(X,\tau) = &- \partial_X \left\{ \left[\frac{\Sigma V}{N\gamma}(T_p^5 - X^{5/2}) + \frac{1}{N} j^{(1)(X)} + \frac{1}{N^2} j^{(2)}(X) \right] F(X,\tau) \right\} \\ &+ \partial_X^2 \left\{ \left[\frac{10\Sigma V T_p^3}{2N^2\gamma^2} + \frac{1}{N^2}\Delta(X) \right] F(X,\tau) \right\}. \end{aligned} \tag{5.23}$$

The corrections to the drift $j^{(1)}$, $j^{(2)}$ and diffusion Δ depend on whether one is using the Floquet model (4.6) or the weak drive model (4.4). Figure 5.2, from Article III, compares steady state-distribution of the temperature of the calorimeter obtained by direct numerical integration from the analytic approximation (5.23). As found in Section 4.1, both equations give matching predictions for $2g^2 \lesssim \kappa$.

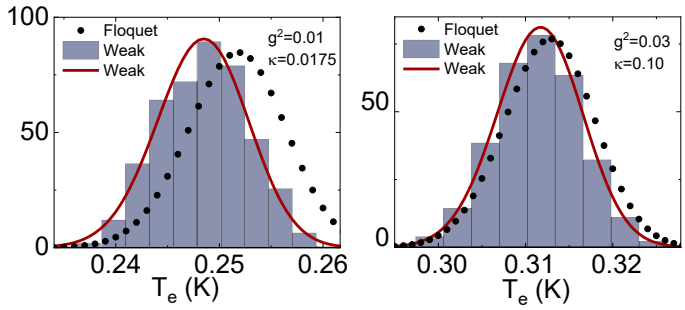

Figure 5.2: Comparison of the steady-state temperature distribution obtained from numerical integration and analytical approximations for different values of the system-bath coupling strength g^2 and driving strength κ. The blue histogram displays the result of numerically integrating (4.4). The full red line shows the prediction of the approximation (5.23) for both weak-drive dynamics and the black dots for the Floquet dynamics. The physical parameters used in the numerical integration are $\hbar\omega = 0.5k_B \times 1$ K, is $V = 10^{-21}\mathrm{m}^3$, $\Sigma = 2 \times 10^{-9}$ W $\mathrm{K}^{-5}\mathrm{m}^{-3}$ and $\gamma = 1500k_B/(1\mathrm{K})$. Source: Article III.

Chapter 6

First Principle Derivation of a Hybrid Master Equation

In this chapter we present a first principle derivation of a hybrid master equation for the state of a system and the energy of the reservoir. We consider a fermion, the central fermion, linearly coupled to a fermion reservoir. This model is quadratic in the system and reservoir operators and therefore the dynamics can be integrated exactly. We present a general formalism to derive the master equation and consider two limits which lead to an explicit equation. By considering weak system reservoir coupling we recover a hybrid master equation of the form that was studied in [84, 85, 86, 22] and in Article III and discussed in Chapter 4. Additionally, we study the limit in which the reservoir has zero energy, i.e. the zero temperature limit.

6.1 Model

We consider a fermion, which we call the central fermion, in contact with a fermion bath. For simplicity we set $\hbar = 1$. The central fermion has energy ω_0, its Hamiltonian is given in terms of the fermionic ladder operators $a^\dagger$, a

$$H_C = \omega_0 a^\dagger a. \tag{6.1}$$

The reservoir Hamiltonian is

$$H_R = \sum_k \omega_k b_k^\dagger b_k, \tag{6.2}$$

where $b_k^\dagger$ and b_k are fermionic ladder operators. Finally, both systems interact linearly as described by

$$H_I = \sum_k g_k (a^\dagger b_k + b_k^\dagger a). \tag{6.3}$$

The total Hamiltonian is the sum of the above three terms

$$H = H_C + H_R + H_I. \tag{6.4}$$

At initial time $t = 0$, the energy of the reservoir is measured, but the measurement outcome forgotten. Let the total system be in a general state ρ_{C+R} before the initial energy measurement and P_E be the projector on the energy state E of the reservoir. An energy E is measured with probability

$$p(E) = \mathrm{tr}\left(P_E \rho_{C+R}\right). \tag{6.5}$$

After measuring E, the total system is in the state

$$\rho_{C+R} \to \tilde{\rho}_{C+R}(E) = \frac{\rho_C(E)}{p(E)} \otimes P_E \tag{6.6}$$

where we defined the central-fermion state by the partial trace tr_R over the reservoir degrees of freedom

$$\rho_C(E) = \frac{1}{n(E)} \mathrm{tr}_B \left(P_E \rho_{C+R}\right) \tag{6.7}$$

and $n(E) = \mathrm{tr}(P_E)$. Note that $\mathrm{tr}_C\, \rho_C(E) = p(E)/n(E)$, ensuring that $\mathrm{tr}\, \rho_{C+R}(E) = 1$. Since the measurement outcome is forgotten, the state after the measurement is given by the sum of all possible outcomes weighted by their probability

$$\begin{aligned} \rho_{C+R} \to \bar{\rho}_{C+R} &= \sum_E p(E) \tilde{\rho}_{C+R}(E) \\ &= \sum_E \rho_C(E) \otimes P_E. \end{aligned} \tag{6.8}$$

This initial condition includes the more common factorised initial state where the reservoir is in a thermal state $\rho_C \otimes e^{-\beta H_B}/\mathrm{tr}(e^{-\beta H_B})$ by taking

$$\rho_C(E) = \rho_C \frac{e^{-\beta E}}{\mathrm{tr}(e^{-\beta H_B})}. \tag{6.9}$$

Following the above discussion our aim is to calculate the partial trace

$$\rho_C(E,\tau) = \mathrm{tr}_R \left(P_E U(\tau) \left(\sum_E \rho_C(E) \otimes P_E \right) U^\dagger(\tau) \right) \tag{6.10}$$

which is the state of the central fermion given a bath energy E. Its trace

$$P(E,\tau) = \mathrm{tr}_C\, \rho_C(E,\tau) \tag{6.11}$$

is the probability for the bath to have energy E at a time τ. It is straightforward to check that $\sum_E P(E,\tau) = 1$.

For our upcoming calculations, it is convenient to express the energy projectors in terms of their Fourier transforms. Let us define

$$\hat{\rho}(\nu_f,\nu_i,\tau) = \mathrm{tr}_B \left(e^{-i\nu_f H_B} U(\tau) \hat{\rho}_C(\nu_i) \otimes e^{i\nu_i H_B} U^\dagger(\tau) \right), \tag{6.12}$$

such that

$$\rho_C(E,\tau) = \int d\nu_f d\nu_i e^{iE\nu_f} \hat{\rho}(\nu_f,\nu_i,\tau). \tag{6.13}$$

It is possible to show that $\int d\nu_i\ \mathrm{tr}_C\, \hat{\rho}(\nu_f,\nu_i,\tau)$ satisfies Bochner's theorem [99] which guarantees that it is the characteristic function of a probability distribution.

6.2 Path Integral formulation

The Fourier transformed density matrix (6.12) can be represented as a standard fermionic path integral over Grassmannian central fermion fields $\phi^\pm(t)$ and reservoir fields $\psi^\pm(t)$ [100, 101, 55]. We define the propagator depending on Grassmann variables η, χ as

$$\Phi(\chi_i,\bar{\chi}_f,\bar{\eta}_i,\eta_f) = \int \left(\prod_k \mathcal{D}(\psi_k^+,\psi_k^-) \right) \mathcal{D}(\phi^+,\phi^-) e^{iS}, \tag{6.14}$$

such that the Fourier transformed density matrix (6.12) is given by

$$\hat{\rho}(\nu_f,\nu_i,\tau) = \int \mu(d\chi_i d\chi_f d\eta_i d\eta_f) \Phi(\chi_i,\bar{\chi}_f,\bar{\eta}_i,\eta_f,\tau) |\chi_f\rangle\langle\bar{\eta}_f|\, \langle\bar{\chi}_i|\hat{\rho}_C(\nu_i)|\eta_i\rangle \tag{6.15}$$

with the integration measure

$$\mu(d\chi) = d\chi d\bar{\chi}\, e^{-\bar{\chi}\chi}. \tag{6.16}$$

The action S has the form

$$\begin{aligned} iS &= iS_C + iS_{CR} + iS_B \\ &+ \sum_k \bar{\psi}_k^+(\tau_0)(e^{i\nu_i\omega_k}\psi_k^-(\tau_0) - \psi_k^+(\tau_0)) - \sum_k \bar{\psi}_k^-(\tau)(e^{-i\nu_f\omega_k}\psi_k^+(\tau) + \psi_k^-(\tau)) \\ &+ \bar{\phi}^-(\tau)(\eta_f - \phi^-(\tau) + \bar{\chi}_f\phi^+(\tau) + \bar{\phi}^+(\tau_0)(\chi_i - \phi^+(\tau_0)) + \bar{\eta}_i\phi^-(\tau_0), \end{aligned} \tag{6.17}$$

where the second line contains the reservoir boundary terms and all ν_i, ν_f dependence, the final line has the central-fermion boundary terms. The free central fermion action is given by

$$S_C = \int_0^\tau dt\, [\bar{\phi}^+(t)(i\partial_t - \omega_0)\phi^+(t) - \bar{\phi}^-(t)(i\partial_t - \omega_0)\phi^-(t)], \tag{6.18}$$

similarly the free bath action is

$$S_B = \int_0^\tau dt \sum_k [\bar{\psi}_k^+(t)(i\partial_t - \omega_k)\psi_k^+(t) - \bar{\psi}_k^-(t)(i\partial_t - \omega_k)\psi_k^-(t)] \tag{6.19}$$

and the central fermion-fermion interaction is described by

$$\begin{aligned} S_{CB} = &- \int_0^\tau \sum_k g_k(\bar{\phi}^+(t)\psi_k^+(t) + \bar{\psi}_k^+(t)\phi^+(t)) \\ &+ \int_{\tau_0}^\tau \sum_k g_k(\bar{\phi}^-(t)\psi_k^-(t) + \bar{\psi}_k^-(t)\phi^-(t)). \end{aligned} \tag{6.20}$$

6.2.1 Integrating the reservoir dynamics

By performing the reservoir path-integrals, we are able to express the propagator Φ in terms of a path integral solely over the central-fermion fields $\phi^\pm$

$$\Phi(\chi_i, \bar{\chi}_f, \bar{\eta}_i, \eta_f) = \prod_k (e^{-i\omega_k(\nu_f - \nu_i)} + 1) \int \mathcal{D}(\phi^+, \phi^-) e^{i\bar{S}}. \tag{6.21}$$

The first factor on the right hand side of the above equation is due to the functional determinant when performing the reservoir path integral. The modified central fermion action is

$$\begin{aligned} i\bar{S} =& iS_C + iS_I + \bar{\phi}^+(\tau_0)(\chi_i - \phi^+(\tau_0)) + \bar{\eta}_i\phi^-(\tau_0) \\ &+ \bar{\phi}^-(\tau)(\eta_f - \phi^-(\tau)) + \bar{\chi}_f\phi^+(\tau), \end{aligned} \tag{6.22}$$

with the correction S_I to the free dynamics

$$iS_I = \int_0^\tau dtds \sum_k g_k^2\, e^{-i\omega_k(t-s)} \begin{pmatrix} \bar{\phi}^+(t) \\ \bar{\phi}^-(t) \end{pmatrix}^T M_k(\nu_f, \nu_i) \begin{pmatrix} \phi^+(s) \\ \phi^-(s) \end{pmatrix} \tag{6.23}$$

and

$$M_k(\nu_f, \nu_i) = \begin{pmatrix} \frac{e^{i\omega_k(\nu_i-\nu_f)}}{e^{i\omega_k(\nu_i-\nu_f)}+1} - \theta(t-s) & \frac{e^{i\omega_k\nu_i}}{e^{i\omega_k(\nu_i-\nu_f)}+1} \\ -\frac{e^{-i\omega_k\nu_f}}{e^{i\omega_k(\nu_i-\nu_f)}+1} & \theta(t-s) - \frac{1}{e^{i\omega_k(\nu_i-\nu_f)}+1} \end{pmatrix}. \tag{6.24}$$

The correction due to interactions S_I is time non-local and contains cross terms between the forward ϕ^+ and the backward contour ϕ^-.

6.2.2 Integrating the central fermion dynamics

In order to formally solve the central-fermion path integrals, let us write $\phi = \varphi + \delta\varphi$ where φ, $\bar{\varphi}$ are classical solutions to the saddle point equations

$$\frac{\delta}{\delta\bar{\varphi}}\bar{S}[\varphi, \delta\bar{\varphi}] = 0 \quad \text{and} \quad \frac{\delta}{\delta\varphi}\bar{S}[\delta\varphi, \bar{\varphi}] = 0. \tag{6.25}$$

Explicitly, the central-fermion saddle-point equations are

$$\begin{aligned} \partial_t\varphi^+(t) =& -i\omega_0\varphi^+(t) - \sum_k |g_k|^2 \int_0^t ds\, e^{-i\omega_k(t-s)}\varphi^+(s) \\ &+ \sum_k |g_k|^2 \int_0^\tau ds\, e^{-i\omega_k(t-s)} \frac{e^{i\omega_k\nu_i}}{e^{-i\omega_k(\nu_f-\nu_i)}+1} \left(e^{-i\omega_k\nu_f}\varphi^+(s) + \varphi^-(s) \right) \end{aligned} \tag{6.26a}$$

$$\begin{aligned} \partial_t\varphi^-(t) =& -i\omega_0\varphi^-(t) - \sum_k |g_k|^2 \int_0^t ds\, e^{-i\omega_k(t-s)}\varphi^-(s) \\ &+ \sum_k |g_k|^2 \int_0^\tau ds\, e^{-i\omega_k(t-s)} \frac{1}{e^{-i\omega_k(\nu_f-\nu_i)}+1} \left(e^{-i\omega_k\nu_f}\varphi^+(s) + \varphi^-(s) \right), \end{aligned} \tag{6.26b}$$

with boundary conditions (6.22)

$$\varphi^+(\tau_0) = \chi_i \quad \text{and} \quad \varphi^-(\tau) = \eta_f \tag{6.27}$$

induced by the boundary terms in the action $\bar{S}$. The action in terms of the classical solutions is

$$\begin{aligned}\bar{S}[\bar{\varphi} + \delta\bar{\varphi}, \varphi + \delta\varphi] =& \bar{S}[\bar{\varphi}, \varphi] + (S_C + S_I)[\delta\bar{\varphi}, \delta\varphi] \\ &- \delta\bar{\varphi}^+\delta\varphi^+ - \delta\bar{\varphi}^-\delta\varphi^-\end{aligned} \tag{6.28}$$

and accordingly the propagator

$$\begin{aligned}&\Phi(\chi_i, \bar{\chi}_f, \bar{\eta}_i, \eta_f) \\ &\quad = e^{i\bar{S}[\bar{\varphi},\varphi]} \int \mathcal{D}(\delta\varphi^+, \delta\varphi^-) e^{i(S_C+S_I)[\delta\bar{\varphi},\delta\varphi] - \delta\bar{\varphi}^+\delta\varphi^+ - \delta\bar{\varphi}^-\delta\varphi^-}\end{aligned} \tag{6.29}$$

The solutions to the saddle point equations are of the form

$$\varphi^+(t) = K^{++}(\nu_f, \nu_i, t)\chi_i + K^{+-}(\nu_f, \nu_i, t)\eta_f \tag{6.30a}$$

$$\varphi^-(t) = K^{-+}(\nu_f, \nu_i, \tau - t)\chi_i + K^{--}(\nu_f, \nu_i, \tau - t)\eta_f \tag{6.30b}$$

with on the one hand $K^{++}(\nu_f, \nu_i, 0) = K^{--}(\nu_f, \nu_i, 0) = 1$ and on the other $K^{+-}(\nu_f, \nu_i, 0) = 0$, $K^{+-}(\nu_f, \nu_i, 0) = 0$, in order to satisfy the boundary conditions (6.27). Using the above expressions for φ we find that

$$\bar{S}[\bar{\varphi}, \varphi] = \begin{pmatrix} \bar{\chi}_f \\ \bar{\eta}_i \end{pmatrix}^T K(\nu_f, \nu_i, t) \begin{pmatrix} \chi_i \\ \eta_f \end{pmatrix} \tag{6.31}$$

with the matrix K

$$K(\nu_f, \nu_i, \tau) = \begin{pmatrix} K^{++}(\nu_f, \nu_i, \tau) & K^{+-}(\nu_f, \nu_i, \tau) \\ K^{-+}(\nu_f, \nu_i, \tau) & K^{--}(\nu_f, \nu_i, \tau) \end{pmatrix}. \tag{6.32}$$

Performing the remaining path integral in (6.29) gives the functional determinant N^{-1} related to integration over a Gaussian measure

$$\frac{1}{N(\nu_f, \nu_i, t)} = \int \mathcal{D}(\delta\varphi^+, \delta\varphi^-) e^{i(S_C+S_B)[\delta\bar{\varphi},\delta\varphi] - \delta\bar{\varphi}^+\delta\varphi^+ - \delta\bar{\varphi}^-\delta\varphi^-} \tag{6.33}$$

Combining equations (6.31) and (6.33), we find that the propagator has the form

$$\Phi(\chi_i, \bar{\chi}_f, \bar{\eta}_i, \eta_f) = \frac{1}{N(\nu_f, \nu_i, \tau)} e^{\begin{pmatrix} \bar{\chi}_f \\ \bar{\eta}_i \end{pmatrix}^T K(\nu_f, \nu_i, \tau) \begin{pmatrix} \chi_i \\ \eta_f \end{pmatrix}}. \tag{6.34}$$

The expression (6.34) for the propagator allows us to express the dynamics of $\rho(\nu_f, \nu_i, \tau)$ in terms of a master equation. Similar to what was done in [102], we differentiate $\rho(\nu_f, \nu_i, \tau)$ with respect to τ and eliminate the dependence on the initial fields χ_i and $\bar{\chi}_i$. The result of this procedure is the master equation

$$\begin{aligned}\partial_\tau \hat{\rho}(\nu_i, \nu_f, \tau) = &\left(\frac{\dot{K}^{++}}{K^{++}} - \frac{\dot{K}^{-+}K^{+-}}{K^{++}K^{--}}\right) a^\dagger a \hat{\rho} + \left(\frac{\dot{K}^{--}}{K^{--}} - \frac{\dot{K}^{-+}K^{+-}}{K^{++}K^{--}}\right) \hat{\rho} a^\dagger a \\ &+ K^{+-}\left(\frac{\dot{K}^{+-}}{K^{+-}} - \frac{\dot{K}^{++}}{K^{++}} - \frac{\dot{K}^{--}}{K^{--}} + \frac{\dot{K}^{-+}(K^{+-})^2}{K^{++}K^{--}}\right) a^\dagger \hat{\rho} a \\ &- \frac{\dot{K}^{-+}}{K^{++}K^{--}} a \hat{\rho} a^\dagger - \left(\frac{\dot{K}^{-+}K^{+-}}{K^{++}} K^{--} - \frac{\dot{N}}{N}\right) \hat{\rho}, \end{aligned} \tag{6.35}$$

where $\dot{K}$ denotes the τ derivative of K. Let us now study two limits which lead to an explicit expression for the hybrid master equation: the weak coupling limit and the zero temperature limit.

6.3 Weak Coupling Master Equation

6.3.1 Weak Coupling Limit

Let us introduce a scaling factor ε to the interaction Hamiltonian

$$H_I \to \varepsilon H_I. \tag{6.36}$$

We can can eliminate the homogeneous term from the saddle point equations (6.26) by defining $\bar{\varphi}^\pm = e^{i\omega_0 t}\varphi^\pm(t)$. Additionally, let us define the kernel

$$\mathcal{K}(t-s) = \sum_k |g_k|^2 e^{-i(\omega_k - \omega)(t-s)} \begin{pmatrix} 1 & 0 \\ 0 & -1 \end{pmatrix} M_k(\nu_f, \nu_i) \tag{6.37}$$

such that the saddle point equations become

$$\partial_t \begin{pmatrix} \bar{\varphi}^+(t) \\ \bar{\varphi}^-(t) \end{pmatrix} = \varepsilon^2 \int_0^\tau ds\, \mathcal{K}(t-s) \begin{pmatrix} \bar{\varphi}^+(s) \\ \bar{\varphi}^-(s) \end{pmatrix}. \tag{6.38}$$

Similar to the procedure outlined in the previous chapter, we introduce a second time scale $\sigma = \varepsilon^2 t$ and write the formal dependence of the fields on both times $\bar{\varphi}^+(t) \to \bar{\varphi}^+(t, \sigma)$. The derivative becomes

$$\partial_t \to \partial_t + \varepsilon^2 \partial_\sigma. \tag{6.39}$$

We assume that the kernel $\mathcal{K}$ only survives for short times, i.e. it only depends on the fast time, such that the integral becomes

$$\int_{\tau_0}^{\tau} ds\, \mathcal{K}(t-s) \begin{pmatrix} \bar{\varphi}^+(s) \\ \bar{\varphi}^-(s) \end{pmatrix} \to \int_{\tau_0}^{\tau} ds\, \mathcal{K}(t-s) \begin{pmatrix} \bar{\varphi}^+(s,\sigma) \\ \bar{\varphi}^-(s,\sigma) \end{pmatrix}. \tag{6.40}$$

The fields thus satisfy the equation

$$(\partial_t + \varepsilon^2 \partial_\sigma) \begin{pmatrix} \bar{\varphi}^+(t,\sigma) \\ \bar{\varphi}^-(t,\sigma) \end{pmatrix} = \varepsilon^2 \int_{\tau_0}^{\tau} ds\, \mathcal{K}(t-s) \begin{pmatrix} \bar{\varphi}^+(s,\sigma) \\ \bar{\varphi}^-(s,\sigma) \end{pmatrix}. \tag{6.41a}$$

Assuming now an expansion of the form

$$\bar{\varphi}^\pm(t,\sigma) = \tilde{\varphi}^\pm(\sigma) + \varepsilon \bar{\varphi}^\pm_{(1)}(t,\sigma) + \frac{\varepsilon^2}{2} \bar{\varphi}^\pm_{(2)}(t,\sigma) + ... \tag{6.41b}$$

where

$$\tilde{\varphi}^\pm(\sigma) = \lim_{t\uparrow\infty,\, \varepsilon^2 t = \text{cte}} \bar{\varphi}^\pm(t,\sigma). \tag{6.41c}$$

We find that the lowest order $\tilde{\varphi}$ satisfies the equation

$$\partial_\sigma \begin{pmatrix} \tilde{\varphi}^+(\sigma) \\ \tilde{\varphi}^-(\sigma) \end{pmatrix} = \int_{\tau_0}^{\tau} ds\, K(t-s) \begin{pmatrix} \tilde{\varphi}^+(\sigma) \\ \tilde{\varphi}^-(\sigma) \end{pmatrix}. \tag{6.42}$$

Let us write the discrete sum over the reservoir modes in (6.26) in terms of the spectral density

$$\sum_k |g_k|^2 \to \int d\omega\, J(\omega) \tag{6.43}$$

and define the integrals

$$\begin{aligned} &\int d\omega\, J(\omega) \int_0^\infty dt\, e^{-i(\omega-\omega_0)(t-s)} \\ &= \int d\omega\, J(\omega) \left(\pi\delta(\omega-\omega_0) - iP\frac{1}{\omega-\omega_0} \right) = \frac{\Gamma}{2} + iS \qquad (6.44a) \\ &\int d\omega\, J(\omega) \int_{-\infty}^\infty dt\, e^{-i(\omega-\omega_0)(t-s)} = \int d\omega\, J(\omega)(2\pi\delta(\omega-\omega_0)) = \Gamma. \qquad (6.44b) \end{aligned}$$

Let us now transform the fields back $\bar{\varphi}^\pm(t) \to e^{i\omega_0 t}\varphi^\pm(t)$ and write equation (6.42) explicitly with the above definitions. The result is

$$\partial_t \varphi^+(t) = -i(\omega_0 + S)\varphi^+(t) - \frac{\Gamma}{2}\varphi^+(t) + \frac{\Gamma/\rho^i}{\rho^f/\rho^i + 1} \left(\rho_f \varphi^+(t) + \varphi^-(t) \right) \tag{6.45a}$$

$$\partial_t \varphi^-(t) = -i(\omega_0 + S)\varphi^-(t) - \frac{\Gamma}{2}\varphi^-(t) + \frac{\Gamma}{\rho^f/\rho^i + 1} \left(\rho^f \varphi^+(t) + \varphi^-(t) \right) \tag{6.45b}$$

with

$$\rho_{f/i} = e^{-i\nu_{i/f}\omega_0}. \tag{6.46}$$

We define the functions

$$u(t) = e^{(-i(\omega_0+S)-\frac{\Gamma}{2})t} \tag{6.47a}$$

$$w(t) = \frac{e^{\Gamma t}(\rho_f/\rho_i + 1)}{\rho_f/\rho_i + e^{\Gamma t}}, \tag{6.47b}$$

such that the solutions to (6.45) are

$$\varphi^+(\tau) = u(\tau)w(\tau)\chi_i + \frac{1}{\rho_f}(w(\tau) - 1)\eta_f \tag{6.48a}$$

$$\varphi^-(0) = \rho_f(u(\tau)w(\tau)\bar{u}(\tau) - 1)\chi_i + \bar{u}(\tau)w(\tau)\eta_f, \tag{6.48b}$$

which gives the components of the K-matrix

$$K(\nu_i, \nu_f, \tau) = \begin{pmatrix} u(\tau)w(\tau) & \frac{1}{\rho_f}(w(\tau) - 1) \\ \rho_f(u(\tau)w(\tau)u^\dagger(\tau) - 1) & u^\dagger(\tau)w(\tau) \end{pmatrix}. \tag{6.49}$$

Note that the form of the matrix K is very similar to form obtained in [102], where the authors performed the partial trace $\mathrm{tr}_B(U(t, t_0)\rho_i \otimes \rho_B U^\dagger(t, t_0))$.

6.3.2 Master equation

Using the explicit form of the matrix K and inverse-Fourier transforming (6.35) up to second order in the coupling strength leads to the hybrid master equation

$$\begin{aligned} \dot{\rho}_C(E, \tau) &= -i(\omega_0 + S)[a^\dagger a, \rho_C(E, \tau)] \\ &+ \Gamma(N_{E+\omega}(\omega)a^\dagger \rho_C(E + \omega, t)a - \frac{\Gamma}{2}N_E(\omega)\{aa^\dagger, \rho_C(E, \tau)\} \\ &+ \Gamma[1 - N_{E-\omega}(\omega)]a\rho_C(E - \omega, \tau)a^\dagger - \frac{\Gamma}{2}[1 - N_E(\omega)]\{a^\dagger a, \rho_C(E, \tau)\} \end{aligned} \tag{6.50}$$

where $N_E(\omega)$ is occupation of modes with energy ω when the bath has energy E

$$N_E(\omega) = \frac{\mathrm{tr}_B(P_E b_\omega^\dagger b_\omega)}{\mathrm{tr}_B(P_E)}. \tag{6.51}$$

Note that in the derivation of (6.50), the last term diagonal in ρ in (6.35) cancels. In the upcoming manuscript this is explicitly demonstrated using Forman's theorem [103, 104, 105, 106, 107] to evaluate the functional determinant N. The cancellation can also be inferred by recalling that $\mathrm{tr}_C\, \hat{\rho}(\nu_f, \nu_i, \tau)$ satisfies Bochner's

theorem and therefore is the characteristic function of a probability distribution. As shown below, equation (6.50) preserves normalisation and positivity of the probability and therefore the final term in (6.35) must vanish. The positivity is checked by taking the trace tr_C on both sides of (6.50), the right hand side is > 0 if $P(E,t) = 0$. To check the preservation of the norm, we suppose that the ground state of the bath has zero energy. Taking the partial trace tr_C of the right hand side of (6.50) and integrating over the energy $\int_0^\infty dE$ leads to

$$\begin{aligned} &- \int_0^\omega dE\, N_E(\omega)\, \mathrm{tr}_C(aa^\dagger \rho_C(E,\tau)) \\ &+ \int_0^\omega dE\, [1 - N_{E-\omega}(\omega)]\, \mathrm{tr}_C(a^\dagger a \rho_C(E-\omega,\tau)). \end{aligned} \tag{6.52}$$

The first line is zero because $N_{E<0}(\omega) = 0$, the second line is zero since $\rho_C(E < 0,\tau) = 0$.

6.4 Zero temperature limit

Let us now consider the specific initial distribution where the bath is pinned at zero energy. This initial condition can be expressed by choosing an initial fermion-reservoir state

$$\tilde{\rho}_{C+R} = \rho_C \otimes \frac{e^{-\beta H_R}}{\mathrm{tr}_R(e^{-\beta H_R})} \tag{6.53}$$

and taking the zero temperature limit $\beta \to \infty$. For our upcoming calculations, this formulation is more convenient so we replace the inverse Fourier transform over ν_i in equation (6.13) by the zero temperature limit

$$\begin{aligned} &\int d\nu_i\, \mathrm{tr}_B \left(e^{-i\nu_f H_B} U(\tau,\tau_0) \left(\hat{\rho}_C(\nu_i) \otimes e^{i\nu_i H_B} \right) U^\dagger(\tau,\tau_0) \right) \\ &= \lim_{\beta\to\infty} \mathrm{tr}_B \left(e^{-i\nu_f H_B} U(\tau,\tau_0) \left(\hat{\rho}_C \otimes e^{-\beta H_B} \right) U^\dagger(\tau,\tau_0) \right). \end{aligned} \tag{6.54}$$

In zero-temperature limit the interaction part S_I (6.23) of the action simplifies significantly

$$\begin{aligned} S_I[\phi^\pm] = -i \int_{\tau_0}^{\tau} dt ds \sum_k |g_k|^2 e^{-i\omega_k(t-s)} &\begin{pmatrix} \bar{\phi}^+(t) \\ \bar{\phi}^-(t) \end{pmatrix}^T \\ &\times \begin{pmatrix} -\theta(t-s) & 0 \\ -\rho_k^f & -\theta(s-t) \end{pmatrix} \begin{pmatrix} \phi^+(s) \\ \phi^-(s) \end{pmatrix}. \end{aligned} \tag{6.55}$$

With this simplification, the solutions to the saddle point equations (6.26) can be expressed in terms of the function $x(t)$, which solves

$$\partial_t x(t) = -i\omega_0 x(t) - \int d\omega J(\omega) \int_0^t ds\, e^{-i\omega(t-s)} x(s) \tag{6.56}$$

where $J(\omega)$ is the spectral density introduced in (6.43). The solutions are

$$\varphi^+(\tau) = x(\tau)\chi_i \tag{6.57a}$$

$$\varphi^-(\tau) = \bar{x}(\tau - t)\eta_f + \int d\omega J(\omega) \int_0^\tau d\sigma d\lambda\, \bar{x}(\tau - \sigma) e^{-i\omega(\sigma+\nu-\gamma)} x(\tau - \gamma)\chi_i \tag{6.57b}$$

such that the K-matrix is

$$K(\tau, \nu) = \begin{pmatrix} x(\tau) & 0 \\ \int d\omega\, J(\omega) e^{-i\nu\omega} D(\tau, \omega) & \bar{x}(\tau) \end{pmatrix} \tag{6.58}$$

with

$$D(\tau, \omega) = \int_0^\tau d\sigma d\lambda\, \bar{x}(\tau - \sigma) e^{-i\omega(\sigma-\gamma)} x(\tau - \gamma). \tag{6.59}$$

With the explicit form of the K-matrix (6.58), it is straightforward to inverse-Fourier transform (6.35). The resulting master equation is

$$\begin{aligned} \dot{\rho}_C(E, \tau) &= -i\Omega_0(\tau)[a^\dagger a, \rho_C(E, \tau)] \\ &+ \int d\omega J(\omega) \frac{\partial_\tau D(\tau, \omega)}{\bar{x}(\tau) x(\tau)} a \rho_C(E - \omega, \tau) a^\dagger - \frac{\gamma(\tau)}{2} \{a^\dagger a, \rho_C(E, \tau)\} \end{aligned} \tag{6.60}$$

where we defined the frequency

$$\Omega_0(\tau) = \frac{1}{2}(\partial_\tau x(\tau)) x^{-1}(\tau) - (\partial_\tau \bar{x}(\tau)) \bar{x}^{-1}(\tau) \tag{6.61}$$

and the rate

$$\gamma(\tau) = -[(\partial_\tau x(\tau)) x^{-1}(\tau) + (\partial_\tau \bar{x}(\tau)) \bar{x}^{-1}(\tau)]. \tag{6.62}$$

Note that the rate is time dependent and not necessarily positive definite.

Similarly as in the weak-coupling case, the final term in equation (6.35) is zero. In this case it is due to the fact that $K^{+-} = 0$ and the function determinant N is constant in time. This can be checked using Forman's theorem [103, 104, 105, 106, 107], or as before inferred since one can check that the equation is

probability conserving by tracing over the central fermion degrees of freedom and by integrating over energy $\int_{-\infty}^{\infty} dE$. The last line of the master equation (6.60) cancels because

$$\int d\omega\, J(\omega) D(\tau, \omega) = 1 - \bar{x}(\tau) x(\tau), \tag{6.63}$$

such that

$$\int d\omega J(\omega) \frac{\partial_\tau D(\tau, \omega)}{\bar{x}(\tau) x(\tau)} = \gamma(\tau). \tag{6.64}$$

Equation (6.63) can be checked by integrating $p(\tau, s) = \bar{x}(\tau - s)x(\tau - s)$ from 0 to τ and using (6.56).

Let us now consider a Lorentzian spectral density

$$J(\omega) = \frac{\Gamma d^2/2\pi}{(\omega - \epsilon)^2 + d^2}. \tag{6.65}$$

For this spectral density we find that

$$\int d\omega J(\omega) e^{-i\omega(t-s)} = \frac{\Gamma d}{2} \exp(-d|t - s| - \epsilon(t - s)). \tag{6.66}$$

Figure 6.1 shows the rate $\gamma(\tau)$ (6.62) as a function of time. Initially the rate is positive indicating that energy will flow from the central fermion to the bath. At later times the rate turns negative, energy will flow back into into the central fermion not because of thermal activation but due to memory effects. For very long times, the rate relaxes to a constant value. Figure 6.2 displays this energy behaviour, additionally we show the probability for the central fermion to be in the up state.

The authors of [43] showed how master equations with non-positive definite rates such as (6.60) can still be unravelled as jump processes. Jumps with negative rates allow the system to jump back to a former state. These jumps are interpreted as information back flowing from the reservoir into the system. This behaviour is seen in Figure 6.2 as energy flows back into the central fermion, not due to thermal activation but negativity of the rate $\gamma(\tau)$.

6.5 Outlook

In this chapter we present a formalism to derive a system-reservoir energy hybrid master equation from first principles. We study the zero temperature and weak

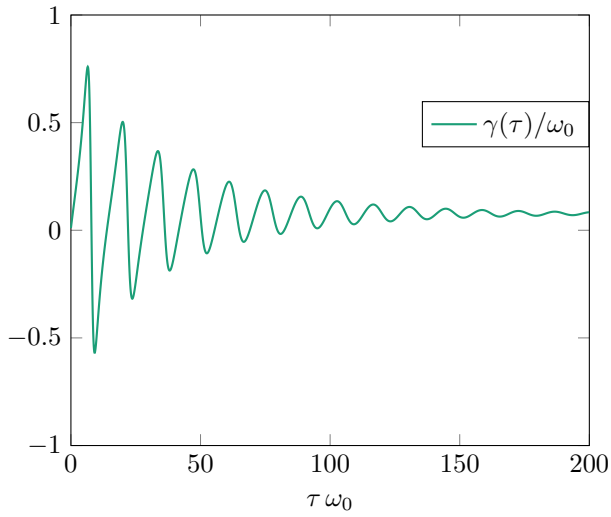

Figure 6.1: The rate $\gamma(\tau)$ (6.62) for a Lorentzian spectral density (6.65). The parameters used are $d = 0.1\omega_0$, $\epsilon = 1.1\omega_0$ and $\Gamma = \omega_0$.

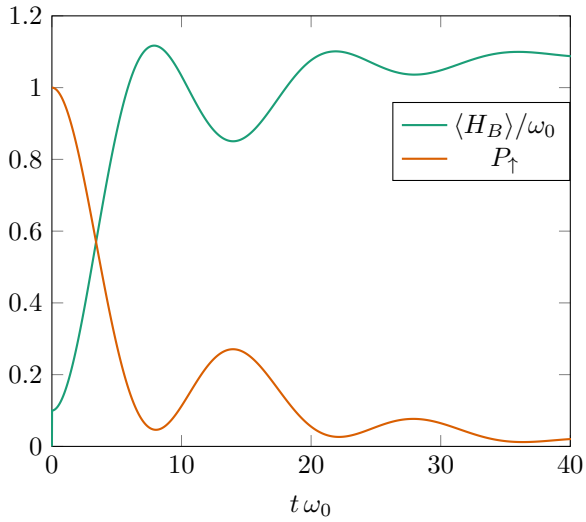

Figure 6.2: Expected energy of the bath as a function of time. The initial state of the central fermion-fermion bath is $|1\rangle\langle 1| \otimes e^{-\beta H_B}$, with $\beta = 10/\omega_0$. The parameters are the same as those in Figure 6.1.

coupling limits for which we obtain an explicit form of the hybrid master equation. In the manuscript in preparation on which this chapter is based, we will present a general hybrid master equation valid at arbitrary system-reservoir coupling and non-zero temperature.

This general hybrid master equation allows us to study various experimentally relevant situations beyond the weak coupling limit. One example, motivated by recent experiments [80, 81], is to study the heat flowing through the fermion when it is coupled to one or more baths. We can also study calorimetric two-measurement thermodynamics similar to the scheme proposed in [18].

The dynamics of strongly coupled systems can exhibit non-Markovian dynamics. With a strong-coupling hybrid master equation we are able to express the non-Markovianity in terms a measurable quantity, the energy of the bath. In the zero temperature limit Figures 6.1 and 6.2 show clear signs of non-Markovianity. The decay rate $\gamma(\tau)$ can turn negative, effectively reversing the direction of the energy flow and causing the central fermion to regain energy from the bath.

Finally we are able to study differences between central fermion and central boson models. The question is whether, beyond weak coupling, we are able to detect distinct signatures of their different statistics.

Chapter 7

Summary

This dissertation reports on the research performed by the author during his doctoral studies. It provides an introduction to Articles I-IV and additionally covers new results in Chapter 6, which is the subject of an article in an advanced stage of preparation. The theoretical research is motivated by recent experimental developments which allow for the study of quantum effects in solid state devices. Specifically, the studies we present are focussed on heat currents and calorimetric measurements in quantum integrated circuits.

Chapter 2 provides a short introduction to weak and strong coupling methods for open quantum systems. Related to strong coupling, the results of Article IV are discussed. In this article the generating function for a driven spin-boson system is derived under the so-called non-interacting blip approximation.

We discuss the Floquet description of driven quantum systems in Chapter 3. We provide an introduction to earlier results and discuss the contribution of the author in Article I to extend an equivalence between Floquet systems and dressed oscillators to open strongly-driven systems.

Chapter 4 deals with calorimetric measurements in quantum integrated circuits. We discuss a specific experimental setup and earlier theoretical studies on this setup. Additionally, we present concrete numerical predictions for the experiment [18] reported in Articles II & III.

In Chapter 5 we introduce the technique of multiscale perturbation theory via a motivating example. We show how in Articles II & III this technique is used predict the steady-state properties of the setup [18].

In Chapter 6 we present new results of the derivation of a hybrid master equation for the state of a system and the energy of a reservoir. We study a fermion linearly coupled to a fermion bath, this quadratic model is integrable

and allows us to extend the description of the setup in Chapter 4 to strong system-reservoir coupling.

References

[1] B. Donvil, L. Ulčakar, T Rejec, and A Ramšak. Thermal effects on a nonadiabatic spin-flip protocol of spin-orbit qubits. *arXiv:2002.05548*, 2020. (submitted).

[2] V. Bouchiat, D. Vion, P. Joyez, D. Esteve, and M. H. Devoret. Quantum coherence with a single cooper pair. *Phys. Scr.*, (T76):165, 1998.

[3] Y. Nakamura, Yu. A. Pashkin, and J. S. Tsai. Coherent control of macroscopic quantum states in a single-cooper-pair box. *Nature*, 398(6730):786–788, April 1999.

[4] M. H. Devoret, A. Wallraff, and J. M. Martinis. Superconducting qubits: A short review, 2004.

[5] Frank Arute, Kunal Arya, Ryan Babbush, Dave Bacon, Joseph C. Bardin, Rami Barends, Rupak Biswas, Sergio Boixo, Fernando G. S. L. Brandao, David A. Buell, Brian Burkett, Yu Chen, Zijun Chen, Ben Chiaro, Roberto Collins, William Courtney, Andrew Dunsworth, Edward Farhi, Brooks Foxen, Austin Fowler, Craig Gidney, Marissa Giustina, Rob Graff, Keith Guerin, Steve Habegger, Matthew P. Harrigan, Michael J. Hartmann, Alan Ho, Markus Hoffmann, Trent Huang, Travis S. Humble, Sergei V. Isakov, Evan Jeffrey, Zhang Jiang, Dvir Kafri, Kostyantyn Kechedzhi, Julian Kelly, Paul V. Klimov, Sergey Knysh, Alexander Korotkov, Fedor Kostritsa, David Landhuis, Mike Lindmark, Erik Lucero, Dmitry Lyakh, Salvatore Mandrà, Jarrod R. McClean, Matthew McEwen, Anthony Megrant, Xiao Mi, Kristel Michielsen, Masoud Mohseni, Josh Mutus, Ofer Naaman, Matthew Neeley, Charles Neill, Murphy Yuezhen Niu, Eric Ostby, Andre Petukhov, John C. Platt, Chris Quintana, Eleanor G. Rieffel, Pedram Roushan, Nicholas C. Rubin, Daniel Sank, Kevin J. Satzinger, Vadim Smelyanskiy, Kevin J. Sung, Matthew D. Trevithick, Amit Vainsencher,

Benjamin Villalonga, Theodore White, Z. Jamie Yao, Ping Yeh, Adam Zalcman, Hartmut Neven, and John M. Martinis. Quantum supremacy using a programmable superconducting processor. *Nature*, 574(7779):505–510, October 2019.

[6] J. Koch, T. M. Yu, J. Gambetta, A. A. Houck, D. I. Schuster, J. Majer, A. Blais, M. H. Devoret, S. M. Girvin, and R. J. Schoelkopf. Charge-insensitive qubit design derived from the cooper pair box. *Phys. Rev. A*, 76:042319, 2007.

[7] H. E. D. Scovil and E. O. Schulz-DuBois. Three-level masers as heat engines. *Physical Review Letters*, 2(6):262–263, March 1959.

[8] R. Alicki. The quantum open system as a model of the heat engine. *J. Phys. A*, 12(5):L103, 1979.

[9] *Maxwell's Demon: Entropy, Information, Computing (Princeton Series in Physics)*. Princeton University Press, apr 2016.

[10] S. Vinjanampathy and J. Anders. Quantum thermodynamics. *Contemporary Physics*, 57:545, 2016.

[11] J H Shirley. Solution of the schrödinger equation with a hamiltonian periodic in time. *Physical Review B*, 138(4 B):979, 1965.

[12] S. Guérin, F. Monti, J-M. Dupont, and H. R. Jauslin. On the relation between cavity-dressed states, floquet states, rwa and semiclassical models. *J. Phys. A: Gen. Phys.*, 30:7193–7215, 1997.

[13] U. Peskin and N Moiseyev. The solution of the time-dependent schrödinger equation by the (t,t') method: Theory, computational algorithm and applications. *J. Chem. Phys.*, 99:4590, 1993.

[14] P. Pfeifer and R. D. Levine. A stationary formulation of the time-dependent problems in quantum mechanics. *J. Chem. Phys.*, 79:5512, 1983.

[15] A. J. Leggett, S. Chakravarty, A. T. Dorsey, M. P. A. Fisher, A. Garg, and W. Zwerger. Dynamics of the dissipative two-state system. *Rev. Mod. Phys.*, 59:1, 1987.

[16] Lena Nicolin and Dvira Segal. Non-equilibrium spin-boson model: Counting statistics and the heat exchange fluctuation theorem. *The Journal of Chemical Physics*, 135(16):164106, October 2011.

[17] Lena Nicolin and Dvira Segal. Quantum fluctuation theorem for heat exchange in the strong coupling regime. *Physical Review B*, 84(16), October 2011.

[18] J. P. Pekola, P. Solinas, A. Shnirman, and D. V. Averin. Calorimetric measurement of quantum work. *New J. Phys.*, 15:115006, 2013.

[19] D. R. Schmidt, C. S. Yung, and A.N. Cleland. Nanoscale radio-frequency thermometry. *Appl. Phys. Lett.*, 83(5), 2003.

[20] S. Gasparinetti, K. L. Viisanen, O.-P. Saira, T. Faivre, M. Arzeo, M. Meschke, and J. P. Pekola. Fast electron thermometry for ultrasensitive calorimetric detection. *Phys. Rev. Appl*, 3:014007, 2015.

[21] Klaara L Viisanen, Samu Suomela, Simone Gasparinetti, Olli-Pentti Saira, Joachim Ankerhold, and Jukka P Pekola. Incomplete measurement of work in a dissipative two level system. *New Journal of Physics*, 17(5):055014, May 2015.

[22] A. Kupiainen, P. Muratore-Ginanneschi, J. Pekola, and K. Schwieger. Fluctuation relation for qubit-calorimetry. *Phys. Rev. E*, 94:062127, 2016.

[23] Vittorio Gorini, A. Kossakowski, and E. C. G. Sudarshan. Completely positive dynamical semigroups of n-level systems. *Journal of Mathematical Physics*, 17(5):821, 1976.

[24] G. Lindblad. On the generators of quantum dynamical semigroups. *Communications in Mathematical Physics*, 48(2):119–130, June 1976.

[25] H. P. Breuer and F. Petruccione. *The theory of open quantum systems.* Clarendon Press Oxford, 2002.

[26] A Rivas and S. F. Huelga. *Open Quantum System: An Introduction.* Springer, 2012.

[27] Michael A. Nielsen and Isaac L. Chuang. *Quantum Computation and Quantum Information.* Cambridge University Press, 2009.

[28] E. B. Davies. Quantum stochastic processes. *Communications in Mathematical Physics*, 15(4):277–304, December 1969.

[29] E. B. Davies. Quantum stochastic processes II. *Communications in Mathematical Physics*, 19(2):83–105, June 1970.

[30] E. B. Davies. The harmonic oscillator in a heat bath. *Communications in Mathematical Physics*, 33(3):171–186, September 1973.

[31] L. Van Hove. Quantum-mechanical perturbations giving rise to a statistical transport equation. *Physica XXI*, 1955.

[32] A. H. Wilson and G. J. Milburn. Interpretation of quantum jump and diffusion processes illustrated on the bloch sphere. *Phys Rev A*, 47(3), 1993.

[33] Jean Dalibard, Yvan Castin, and Klaus Mølmer. Wave-function approach to dissipative processes in quantum optics. *Physical Review Letters*, 68(5):580–583, February 1992.

[34] Klaus Mølmer, Yvan Castin, and Jean Dalibard. Monte carlo wave-function method in quantum optics. *Journal of the Optical Society of America B*, 10(3):524, March 1993.

[35] Howard Carmichael. *An Open Systems Approach to Quantum Optics*. Springer Berlin Heidelberg, 1993.

[36] R. Dum, P. Zoller, and H. Ritsch. Monte carlo simulation of the atomic master equation for spontaneous emission. *Physical Review A*, 45(7):4879–4887, April 1992.

[37] N. Gisin and I. C. Percival. The quantum-state diffusion model applied to open systems. *Journal of Physics A: Mathematical and General*, 25(21):5677–5691, November 1992.

[38] H. P. Breuer and F. Petruccione. Reduced system dynamics as a stochastic process in hilbert space. *Phys. Rev. Lett.*, 74(19):3788, 1995.

[39] H. P. Breuer and F. Petruccione. Stochastic dynamics of quantum jumps. *Phys. Rev. E*, 52(1):428, 1995.

[40] Ian Percival. *Quantum State Diffusion*. Cambridge University Press, jan 1999.

[41] H. M. Wiseman and G. J. Milburn. *Quantum Measurement and Control*. Cambridge University Press, 2010.

[42] Jürgen T. Stockburger and Hermann Grabert. Exactc-number representation of non-markovian quantum dissipation. *Physical Review Letters*, 88(17), April 2002.

[43] Jyrki Piilo, Sabrina Maniscalco, Kari Härkönen, and Kalle-Antti Suominen. Non-markovian quantum jumps. *Physical Review Letters*, 100(18), May 2008.

[44] S. Haroche and J-M. Raimond. *Exploring the Quantum: Atoms, Cavities and Photons*. Oxford University Press, 2006.

[45] K. Jacobs. *Stochastic Processes for Physicists*. Cambridge University Press, 2010.

[46] C.-F. Li, G.-C. Guo, and J. Piilo. Non-markovian quantum dynamics: What does it mean? *EPL (Europhysics Letters)*, 127(5):50001, October 2019.

[47] C.-F. Li, G.-C. Guo, and J. Piilo. Non-markovian quantum dynamics: What is it good for? *EPL (Europhysics Letters)*, 128(3):30001, January 2020.

[48] P. Deuar and P. D. Drummond. Correlations in a BEC collision: First-principles quantum dynamics with 150 000 atoms. *Physical Review Letters*, 98(12), March 2007.

[49] R Ng and E S Sørensen. Exact real-time dynamics of quantum spin systems using the positive-p representation. *Journal of Physics A: Mathematical and Theoretical*, 44(6):065305, January 2011.

[50] R. P. Feynman. Space-time approach to non-relativistic quantum mechanics. *Reviews of Modern Physics*, 20(2):367–387, April 1948.

[51] R.P Feynman and F.L Vernon. The theory of a general quantum system interacting with a linear dissipative system. *Annals of Physics*, 24:118–173, October 1963.

[52] John R Klauder. The action option and a feynman quantization of spinor fields in terms of ordinary c-numbers. *Annals of Physics*, 11(2):123–168, October 1960.

[53] R. P. Feynman, A. R. Hibbs, and George H. Weiss. Quantum mechanics and path integrals. *Physics Today*, 19(6):89–89, June 1966.

[54] A. Kamenev and A. Levchenko. Keldysh technique and non-linear sigma-model: basic principles and applications. *Adv Phys*, 2009.

[55] A. Altland and B. Simons. *Condensed Matter Field Theory*. Cambridge University Press, 2010.

[56] A. J. Leggett, S. Chakravarty, A. T. Dorsey, Matthew P. A. Fisher, Anupam Garg, and W. Zwerger. Dynamics of the dissipative two-state system. *Reviews of Modern Physics*, 59(1):1–85, jan 1987.

[57] Sudip Chakravarty and Anthony J. Leggett. Dynamics of the two-state system with ohmic dissipation. *Physical Review Letters*, 52(1):5–8, January 1984.

[58] Ulrich Weiss. *Quantum Dissipative Systems*. World Scientific, Singapore, 1993.

[59] Claude Aslangul, Noëlle Pottier, and Daniel Saint-James. Spin-boson systems: equivalence between the dilute-blip and the Born approximations. *Journal de Physique*, 47(10):1657–1661, 1986.

[60] H. Dekker. Noninteracting-blip approximation for a two-level system coupled to a heat bath. *Phys. Rev. A*, 35(3):35, 1987.

[61] Denis J. Evans, E. G. D. Cohen, and G. P. Morriss. Probability of second law violations in shearing steady states. *Physical Review Letters*, 71(15):2401–2404, oct 1993.

[62] G. Gallavotti and E. G. D. Cohen. Dynamical ensembles in nonequilibrium statistical mechanics. *Physical Review Letters*, 74(14):2694–2697, apr 1995.

[63] Jorge Kurchan. Fluctuation theorem for stochastic dynamics. *Journal of Physics A: Mathematical and General*, 31(16):3719–3729, apr 1998.

[64] Christian Maes, Frank Redig, and Annelies Van Moffaert. On the definition of entropy production, via examples. *Journal of Mathematical Physics*, 41(3):1528–1554, mar 2000.

[65] B. Ya. Zeldovich. The quasienergy of a quantum-mechanical system subjected to a periodic action. *Soviet Physics Jetp*, 24(5):1006, 1967.

[66] Gaston Floquet. Sur les eéquations diffeérentielles lineéaires à coefficients peériodiques. *Annales scientifiques de l'É.N.S. 2*, 12:47–88, 1883.

[67] Andrew Stephenson. XX. on induced stability. *The London, Edinburgh, and Dublin Philosophical Magazine and Journal of Science*, 15(86):233–236, February 1908.

[68] P. L. Kapitza. Dynamic stability of a pendulum when its point of suspension vibrates. *Soviet Phys. JETP.*, 21:588, 1951.

[69] Takashi Oka and Sota Kitamura. Floquet engineering of quantum materials. *Annual Review of Condensed Matter Physics*, 10(1):387–408, March 2019.

[70] Krzysztof Sacha and Jakub Zakrzewski. Time crystals: a review. *Reports on Progress in Physics*, 81(1):016401, November 2017.

[71] R. Bümel, A. Buchleitner, R. Graham, L. Sirko, U. Smilansky, and H. Walther. Dynamical localization in the microwave interaction of rydberg atoms: The influence of noise. *Phys. Rev. A*, 44:4521, 1991.

[72] T. Dittrich, B. Oelschlägel, and P. Hänggi. Driven tunneling with dissipation. *Europhys. Lett.*, 1993.

[73] B. Oelschlägel, T. Dittrich, and P. Hänggi. Damped periodically driven quantum transport in bistable systems. *Acta Physica Polonica B*, 4:845, 1993.

[74] M. Grifoni and P. Hänggi. Driven quantum tunneling. *Physics Reports*, 304:229–354, 1998.

[75] S. Gasparinetti, P. Solinas, S. Pugnetti, R. Fazio, and J. P. Pekola. Environment-governed dynamics in driven quantum systems. *Physical Review Letters*, 110(15), April 2013.

[76] Vera Gramich, Simone Gasparinetti, Paolo Solinas, and Joachim Ankerhold. Lamb-shift enhancement and detection in strongly driven superconducting circuits. *Physical Review Letters*, 113(2), July 2014.

[77] H. P. Breuer and F. Petruccione. Dissipative quantum system in strong laser fields: Stochastic wave-function method and floquet theory. *Phys Rev A*, 55(4):3101, 1997.

[78] S. Gasparinetti, P. Solinas, A. Braggio, and M. Sassetti. Heat-exchange statistics in driven open quantum systems. *New J. Phys.*, 16:115001, 2014.

[79] G. Bulnes Cuetara, A. Engel, and M. Esposito. Stochastic thermodynamics of rapidly driven systems. *New J. Phys.*, 17:055002, 2015.

[80] Alberto Ronzani, Bayan Karimi, Jorden Senior, Yu-Cheng Chang, Joonas T. Peltonen, ChiiDong Chen, and Jukka P. Pekola. Tunable photonic heat transport in a quantum heat valve. *Nature Physics*, 14(10):991–995, July 2018.

[81] J. Senior, A. Gubaydullin, B. Karimi, J. Peltonen, J. Ankerhold, and J. Pekola. Heat rectification via a superconducting artificial atom. *arXiv:1908.05574*, 2019.

[82] Bayan Karimi, Danilo NIkolic, Tuomas Tuukkanen, Joonas T. Peltonen, Wolfgan Belzig, and Jukka P. Pekola. Optimized proximity thermometer for ultra-sensitive detection. *arXiv:1911.02844*, 2019.

[83] F. W. J. Hekking and J. P. Pekola. Quantum jump approach for work and dissipation in a two-level system. *Phys Rev Lett*, 111, 2013.

[84] T. L. van den Berg, F. Brange, and P. Samuelsson. Energy and temperature fluctuations in the single electron box. *New J. Phys.*, 17:075012, 2015.

[85] S. Suomela, A. Kutvonen, and T. Ala-Nissila. Quantum jump model for a system with a finite-size environment. *Physical Review E*, 93(6), June 2016.

[86] S. Suomela, R. Sampaio, and T. Ala-Nissila. Comparison between quantum jumps and master equation in the presence of a finite environment. *Physical Review E*, 94(3), September 2016.

[87] Bayan Karimi and Jukka P. Pekola. Quantum trajectory analysis of single microwave photon detection by nanocalorimetry, 2020.

[88] N. W. Ashcroft and D. Mermin. *Solid State Physics*. Saunders College Publishing, Philadelphia, 1st edition, 1976.

[89] M.I. Kaganov, I.M. Lifshitz, and L.V. Tanatarov. Relaxation between electrons and the crystalline lattice. *Soviet Physics Jetp*, 31:232, 1956.

[90] F. C. Wellstood, C. Urbina, and J. Clarke. Hot-electron effects in metals. *Phys. rev. B*, 49:5942, 1994.

[91] Francesco Giazotto, Tero T. Heikkilä, Arttu Luukanen, Alexander M. Savin, and Jukka P. Pekola. Opportunities for mesoscopics in thermometry and refrigeration: Physics and applications. *Reviews of Modern Physics*, 78(1):217–274, March 2006.

[92] L. B. Wang, O.-P. Saira, D. S. Golubev, and J. P. Pekola. Crossover between electron-phonon and boundary-resistance limits to thermal relaxation in copper films. *Physical Review Applied*, 12(2), August 2019.

[93] J. P. Pekola and B. Karimi. Quantum noise of electron-phonon heat current. *J. Low. Temp. Phys.*, 191(5-6):373, 2018.

[94] Roope Kokkoniemi, Joonas Govenius, Visa Vesterinen, Russell E. Lake, András M. Gunyhó, Kuan Y. Tan, Slawomir Simbierowicz, Leif Grönberg, Janne Lehtinen, Mika Prunnila, Juha Hassel, Antti Lamminen, Olli-Pentti Saira, and Mikko Möttönen. Nanobolometer with ultralow noise equivalent power. *Communications Physics*, 2(1), oct 2019.

[95] Bayan Karimi, Fredrik Brange, Peter Samuelsson, and Jukka P. Pekola. Reaching the ultimate energy resolution of a quantum detector. *Nature Communications*, 11(1), jan 2020.

[96] C. M. Bender and S. A. Orszag. *Advanced Mathematical Methods for Scientists and Engineers I.* Springer Science+Business Media, 1999.

[97] G. A. Pavliotis and A. M. Stuart. *Multiscale methods: averaging and homogennization.* Springer, 1 edition, 2008.

[98] S. H. Strogatz. *Nonlinear Dynamics and Chaos.* Addison-Wesley Publishing Company, 1994.

[99] David Stirzaker Geoffrey Grimmett. *Probability and Random Processes.* Oxford University Press, 2001.

[100] Jean Zinn-Justin. *Path Integrals in Quantum Mechanics.* Oxford University Press, November 2004.

[101] Alex Kamenev. *Field Theory of Non-Equilibrium Systems.* Cambridge University Press, 2009.

[102] Matisse W. Y. Tu and Wei-Min Zhang. Non-markovian decoherence theory for a double-dot charge qubit. *Physical Review B*, 78(23), December 2008.

[103] Robin Forman. Functional determinants and geometry. *Inventiones Mathematicae*, 88(3):447–493, oct 1987.

[104] Klaus Kirsten and Alan J. McKane. Functional determinants by contour integration methods. *Annals of Physics*, 308(2):502–527, dec 2003.

[105] Klaus Kirsten and Alan J McKane. Functional determinants for general sturm–liouville problems. *Journal of Physics A: Mathematical and General*, 37(16):4649–4670, apr 2004.

[106] A J McKane and M B Tarlie. Regularization of functional determinants using boundary perturbations. *Journal of Physics A: Mathematical and General*, 28(23):6931–6942, dec 1995.

[107] P. Muratore-Ginanneschi. Path integration over closed loops and gutzwiller's trace formula. *Physics Reports*, 383(5-6):299–397, sep 2003.